ИНСТИТУТ ЯДЕРНОЙ ФИЗИКИ СО АН СССР

A.A. Zholents

BEAM-BEAM EFFECTS IN ELECTRON-POSITRON STORAGE RINGS

PREPRINT 91-18

НОВОСИБИРСК

INTRODUCTION

During the past twenty five years fifteen electron-positron storage rings have been built and commissioned all around the world and a substantial progress in luminosity has been reached. Now a design consideration of a new storage ring is well approved both theoretically and experimentally in all aspects except one. This exception is a problem of the beam-beam interaction, which is a subject of the present paper. Our knowledge here is quite rich, but not at a level of good understanding of the phenomenon. It remains still unexplained why the beam-beam limit is so small for the most existing storage rings.

The lack of the good theory can hardly be compensated and this review of the beam-beam effects is not an exception. A choice of the material for a review and the accents on the relative importance of different questions were done rather by intuition than on some systematic basis. For a more complete study of the beam-beam effects one needs to apply to the additional information. Some of the excellent reviews can be found in the reference list.

1. EVALUATION OF THE BEAM-BEAM KICKS

Here we find the integrated transverse angular deflection received by a particle crossing a charged beam. The coordinate systems used below are shown in the Fig. 1.

We assume that the distribution of the charge, Ne, in the oncoming bunch is Gaussian in all three dimensions.

$$\rho(x,\ y,\ z) = \frac{Ne}{(2\pi)^{3/2}abc} \exp\left\{-\frac{\bar{x}^2}{2a^2} - \frac{\bar{y}^2}{2b^2} - \frac{\bar{z}^2}{2c^2}\right\} \qquad (1.1)$$

where a, b, c are the standard deviations in $\bar{x}$, $\bar{y}$ and $\bar{z}$.

It has been shown [1] that the electric potential produced by this distribution is

$$U(\bar{x},\ \bar{y},\ \bar{z}) = \frac{Ne}{\sqrt{\pi}} \int_0^\infty \frac{\exp\left\{\frac{\bar{x}^2}{2a^2+t} - \frac{\bar{y}^2}{2b^2+t} - \frac{\bar{z}^2}{2c^2+t}\right\} dt}{[(2a^2+t)(2b^2+t)(2c^2+t)]^{1/2}}. \qquad (1.2)$$

For a convenience of the reader we present the evaluation of the potential in the appendix. The transverse electric and magnetic fields of this bunch moving with the speed of light c along z-axis are given by:

$$E_x = -\gamma \frac{\partial U}{\partial x} = \frac{2Ne}{\sqrt{\pi}} \gamma x \times$$

$$\int_0^\infty dt \frac{\exp\left\{-\frac{x^2}{2\sigma_x^2+t} - \frac{y^2}{2\sigma_y^2+t} - \frac{\gamma^2(z+c\tau)^2}{\gamma^2 2\sigma_z^2+t}\right\}}{(2\sigma_x^2+t)[(2\sigma_x^2+t)(2\sigma_y^2+t)(\gamma^2 2\sigma_z^2+t)]^{1/2}}, \qquad (1.3)$$

$$E_y = -\gamma \frac{\partial U}{\partial y} = \frac{2Ne}{\sqrt{\pi}} \gamma y \times$$

$$\int_0^\infty dt \frac{\exp\left\{-\frac{x^2}{2\sigma_x^2+t} - \frac{y^2}{2\sigma_y^2+t} - \frac{\gamma^2(z+c\tau)^2}{\gamma^2 2\sigma_z^2+t}\right\}}{(2\sigma_y^2+t)[(2\sigma_x^2+t)(2\sigma_y^2+t)(\gamma^2 2\sigma_z^2+t)]^{1/2}}. \qquad (1.4)$$

$$H_x = E_y, \qquad (1.5)$$

$$H_y = -E_x, \qquad (1.6)$$

where γ is the Lorentz factor and σ_x, σ_y, σ_z are the standard deviations in the laboratory frame.

It is easy to calculate the transverse kicks by integrating the corresponding component of the Lorentz force over time τ:

$$\Delta x' \equiv \Delta P_x/P = -\int_\infty^\infty d\tau e(E_x - H_y)/P \approx -(2e/\gamma mc)\int_{-\infty}^\infty d\tau E_x, \qquad (1.7)$$

$$\Delta y' \equiv \Delta P_y/P = -\int_\infty^\infty d\tau e(E_y + H_x)/P \approx -(2e/\gamma mc)\int_{-\infty}^\infty d\tau E_y. \qquad (1.8)$$

We assume in the beginning that the variations of σ_x and σ_y with z on the interval of $\pm\sigma_z$ are very weak and find

$$\begin{Bmatrix}\Delta x' \\ \Delta y'\end{Bmatrix} = -\frac{2Nr_e}{\gamma} \begin{Bmatrix}x \\ y\end{Bmatrix} \int_0^\infty dt \frac{\exp\left\{-\frac{x^2}{2\sigma_{x+t}^2} - \frac{y^2}{2\sigma_{y+t}^2}\right\}}{(2\sigma_{x,y+t}^2)[(2\sigma_x^2+t)(2\sigma_y^2+t)]^{1/2}}, \qquad (1.9)$$

where r_e is the classical electron radius.

We consider the beam-beam effects, associated with the finite bunch length, in the section 5.

Equations (1.9) can also be written [2] as

$$\Delta x' = - \frac{Nre}{\gamma} \sqrt{\frac{2\pi}{\sigma_x^2 - \sigma_y^2}}\, Im\, \{F\,(x,\ y)\}, \qquad (1.10)$$

$$\Delta y' = - \frac{Nre}{\gamma} \sqrt{\frac{2\pi}{\sigma_x^2 - \sigma_y^2}}\, Re\, \{F\,(x,\ y)\}, \qquad (1.11)$$

where a condition $\sigma_x > \sigma_y$ is assumed and

$$F\,(x,\ y) = W\left(\frac{x + iy}{\sqrt{2\,(\sigma_x^2 - \sigma_y^2)}}\right) - \exp\left\{-\frac{x^2}{2\sigma_x^2} - \frac{y^2}{2\sigma_y^2}\right\} \times$$

$$W\left(\frac{x\,\frac{\sigma_y}{\sigma_x} + iy\,\frac{\sigma_x}{\sigma_y}}{\sqrt{2\,(\sigma_x^2 - \sigma_y^2)}}\right). \qquad (1.12)$$

Here W ( ) is the complex error function.

In the two extreme cases of a round beam cross-section ($\sigma_x = \sigma_y$) and a very flat beam cross-section ($\sigma_x \gg \sigma_y$) the formulae (1.10) and (1.11) can be simplified significantly. Directly applying the Gauss law for a evaluation of E_x, E_y one can obtain for round beams

$$\Delta r' = - \frac{2Nre}{\gamma} \frac{1}{r} \left[1 - e^{-r^2/2\sigma^2}\right] \qquad (1.13)$$

and for flat beams in the region of $|y| \ll \sigma_x$

$$\Delta x' = \frac{2reN}{\gamma} \frac{\sqrt{2}}{\sigma_x} F_D\,(x/\sqrt{2}\ \sigma_x), \qquad (1.14)$$

$$\Delta y' = \frac{2reN}{\gamma} \frac{i}{\sigma_x} \sqrt{\frac{\pi}{2}}\, e^{-\frac{x^2}{2\sigma x^2}}\, \Phi\,(y/\sqrt{2}\ \sigma_y),$$

where $F_D(z) = e^{-z^2} \int_0^z e^{t^2}\, dt$ is the Dawson function and Φ ( ) is the error function.

2. LINEAR APPROXIMATION

We can already obtain several useful results considering small oscillations with $|x| \ll \sigma_x$ and $|y| \ll \sigma$. Equation (1.9) becomes

$$\Delta x' = - \frac{2Nre}{\gamma\sigma_x\,(\sigma_x + \sigma_y)}\, x,$$

$$\Delta y' = - \frac{2Nre}{\gamma\sigma_y\,(\sigma_x + \sigma_y)}\, y. \qquad (2.1)$$

In this approximation x and y motions are decoupled and we can consider one dimension only. Let it be y dimension.

Due to the linearization the beam-beam kick is equivalent to the effect of a thin quadrupole with the focal length f

$$\frac{1}{f} = \frac{2Nre}{\gamma\sigma_y\,(\sigma_x + \sigma_y)}. \qquad (2.2)$$

The transformation of the $(y,\ y')$ vector through one beam-beam collision to the next is described by the matrix

$$\begin{bmatrix} \cos\,(\mu + \Delta\mu) & \tilde{\beta}\,\sin\,(\mu + \Delta\mu) \\ -\frac{1}{\tilde{\beta}}\,\sin\,(\mu + \Delta\mu) & \cos\,(\mu + \Delta\mu) \end{bmatrix} =$$

$$= \begin{bmatrix} \cos\mu & \beta \sin\mu \\ -\frac{1}{\beta}\sin\mu & \cos\mu \end{bmatrix} \begin{bmatrix} 1 & 0 \\ -\frac{1}{f} & 1 \end{bmatrix}, \qquad (2.3)$$

where β, $\tilde{\beta}$ are unperturbed and perturbed beta-functions at the collision point and μ is the phase advance of betatron oscillations between two interactio

If the perturbed motion is stable, than

$$\cos(\mu + \Delta\mu) = \cos\mu - 2\pi\xi \sin\mu, \qquad (2.4)$$

$$\tilde{\beta} \sin(\mu + \Delta\mu) = \beta \sin\mu,$$

where

$$\xi_{x,y} = \frac{Nr_e \beta_{x,y}}{2\pi\gamma\sigma_{x,y}(\sigma_x + \sigma_y)}. \qquad (2.5)$$

For $\Delta\mu \ll 1$ one can find for a tune shift of the betatron oscillation:

$$\Delta\nu = \xi. \qquad (2.6)$$

Therefore the parameter ξ is often called as linear beam-beam tune shift. The relationship (2.6) is only valid for tune values not too close to the half integer. The exact dependence of $\Delta\nu$ on ξ and μ is shown in Fig. 2 [3].

The evident conclusion from this plot is the following. For a fixed value ξ one can have the benefit to have smaller $\Delta\nu$ if choice the betatron tune slightly above a half-integer.

From the equation (2.4) we can also find [4]

$$\tilde{\beta} = \frac{\beta}{\sqrt{1 + 4\pi\xi \cot\mu - 4\pi^2\xi^2}}. \qquad (2.7)$$

The beam-beam force pinches the beta-function and consequently the beam size at the collision point to a smaller value if $\mu/2\pi < 0.1$. It is so-called effect of the dynamic beta-function [4]. For large $\mu/2\pi$ the reverse is true. This means the luminosity would also benefit from having the betatron tune slightly above a half-integer. Several examples of the dynamic beta behavior are shown in Fig.3.

From considerations above we can figure out a recommendation for choosing betatron tunes slightly above a half integer. Some experimental verification for this rule we find in SPEAR-I data [5] (see Fig. 4). However to follow this strategy is not easy in practice. The cause is single beam synchrobetatron resonances.

Beam-beam strength parameter ξ is much more relevant for a calculation of the luminosity than the number of particles in the bunch N. The maximal ξ value is correspondent to the maximal possible perturbation in the particle motion when it remains stable. Therefore a standard luminosity formula

$$L = f \frac{N^2}{4\pi\sigma_x\sigma_y}, \qquad (2.8)$$

where f is the collision frequency, must be rewritten in the form, including ξ:

$$L = f \frac{N}{2r_e} \frac{\xi_y}{\beta_y} (1 + \sigma_y / \sigma_x). \qquad (2.9)$$

This presentation of the luminosity formula is consistent with the experimental observations of luminosity and ξ behavior with beam intensity for many e^+e^- storage rings. (See, for example, Fig. 5, where CESR data is presented [6]). At low currents the luminosity is proportional to the current squared and the beam sizes are constant. At a certain current the vertical tune shift saturates which forces the beam size product to grow in proportion to the current. Thus, the luminosity also grows linearly with current. Non Gaussian transverse tails develop on the beams and subsequently increase linearly with currents until the aperture limit is reached. At that value the beam lifetime is significantly reduced.

Equally with the parameter ξ the luminosity is determined by three others: crossing frequency, f, vertical beta-function at the interaction point (IP), β_y, and the beam dimensions ratio, $r = \sigma_y/\sigma_x$.

Though the beam-beam subject is usually consider as the dynamics of the beam-beam interaction and concerns the problems of ξ limit, we can not totally pass by these additional parameters. Attempts to increase the luminosity with the use of some of them are very often limited by ξ reduction. Therefore at the appropriate points we shall return to the consideration of these parameters.

Nevertheless, we will be most interested in various possible mechanisms that cause the beam-beam limit.

3. AN ISOLATED RESONANCE IN TWO DEGREES OF FREEDOM

As our first beam-beam picture we consider the two dimensional motion of a single particle interacting with the charged bunch at the collision point and performing free betatron oscillation between the collisions. This is so called 'weak-strong' case. The periodicity of the motion and the nonlinear character of the interaction are the causes of two important effects: an excitation of the nonlinear resonance and tune dependencies from the oscillation amplitude of the particle, which will end up with tune spreads, if a weak beam contains a distribution of particles of various amplitudes.

We begin with the Hamiltonian

$$H = \frac{K_x x^2}{2} + \frac{x'^2}{2} + \frac{K_y y^2}{2} + \frac{y'^2}{2} + V(x, y) \sum_{k=-\infty}^{\infty} \delta(z - kC), \quad (3.1)$$

where K_x, K_y are usual focusing functions, x, x', y, y' are betatron coordinates and canonical momenta, normalized on the standard deviations, σ_x, $\sigma_{x'}$, σ_y, $\sigma_{y'}$, C is the period between interactions and the potential

$$V\ (x,\ y) = \xi_y \frac{\sigma_y}{\beta} \int f_y(x,y)\ dy = \xi_x \frac{\sigma_x}{\beta} \int f_x(x,y)\ dx \quad (3.2)$$

is the perturbation, while f_x, f_y are dimensionless beam-beam forces. In this notation the beam-beam kicks are described in the form

$$\Delta x' = - \xi_x f_x,$$
$$\Delta y' = - \xi_y f_y. \quad (3.3)$$

The transformation of the Hamiltonian (3.1) to action-angle variables $(x,\ x',\ y,\ y') \to (\Phi_x,\ I_x,\ \Phi_y,\ I_y)$ can be accomplished with the generation function

$$F(x,\Phi_x,y,\Phi_y) = \sum_{q=x,y} \frac{-q^2}{2\beta_q} \tan\left[\Phi_q - \frac{2\pi\nu_q s}{C} + \int_0^s \frac{ds'}{\beta_q(s')}\right] + \frac{q^2}{4\beta_q}\beta_q' \quad (3.4)$$

which yields the transformation equations

$$q = \sqrt{2I_q\beta_q}\cos(\Phi_q),$$
$$q' = -\sqrt{2I_q/\beta_q}\left(\sin\Phi_q - \frac{\beta_r'}{2}\cos\Phi_q\right) \quad (3.5)$$

and new Hamiltonian H

$$H_1 = \nu_x I_x + \nu_y I_y + V\ (I_x,\ \Phi_x,\ I_y,\ \Phi_y)\ \delta_{2\pi}(\theta), \quad (3.6)$$

where z has been replaced by a new dimensionless variable $\theta = 2\pi z/C$ and

$$\delta_{2\pi}(\theta) = \sum_{k=-\infty}^{\infty} \cos k\theta. \quad (3.7)$$

Then, the problem can be reduced with the expansion of the potential V in the Fourier series

$$V = \sum_{\ell,m=-\infty}^{\infty} V_{\ell,m} \cos(\ell\Phi_x)\cos(m\Phi_y)$$

and averaging of the Hamiltonian over the 'time' θ. Only two term are retained in the Hamiltonian. They are a phase independent term

$$V_{00} = \frac{1}{(2\pi)^3} \int_0^{2\pi}\int V\ d\Phi_x d\Phi_y \quad (3.8)$$

and a resonant term $V_{\ell m}\cos(\ell\Phi_x + m\Phi_y - k\theta)$, where

$$V_{\ell m} = \frac{1}{(2\pi)^2} \int_0^{2\pi}\int V \cos\ell\Phi_x \cos m\Phi_y\ d\Phi_x d\Phi_y. \quad (3.9)$$

All other Fourier terms are assumed to have phases which oscillate rapidly and can thus be averaged to zero.

Thus we come to the truncated Hamiltonian

$$\langle H_1 \rangle = \nu_x I_x + \nu_y I_y + V_{00} + V_{\ell m}\cos(\ell\Phi_x + m\Phi_y - k\theta). \quad (3.10)$$

The effect of V_{00} is to make the average frequencies of oscillation dependent upon the particle amplitudes defined as

$$A_x = \frac{\sqrt{2I_x\beta_x}}{\sigma_x}; \qquad A_y = \frac{\sqrt{2I_y\beta_y}}{\sigma_y}. \quad (3.11)$$

According to the standard definitions of the nonlinear tune shifts [7]

$$\Delta\nu_x = \frac{\partial V_{00}}{\partial I_x}, \qquad \Delta\nu_y = \frac{\partial V_{00}}{\partial I_y}, \tag{3.12}$$

one can get from the substitution of (3.2) and (3.8) into (3.12)

$$\Delta\nu_x\,(A_x, A_y) = \xi_x \frac{1}{(2\pi)^3 A_x} \int_0^{2\pi}\int f_x \cos\Phi_x \, d\Phi_x d\Phi_y,$$

$$\Delta\nu_y\,(A_x, A_y) = \xi_y \frac{1}{(2\pi)^3 A_y} \int_0^{2\pi}\int f_y \cos\Phi_y \, d\Phi_x d\Phi_y. \tag{3.13}$$

The Hamiltonian (3.10) can be reduced to the one dimensional case by using a canonical transformation to a rotating system in phase space. The generation function of this transformation is

$$F_2(\Phi_x, \Phi_y, K_1, K_2, \theta) = (\ell\Phi_x + m\Phi_y - k\theta)K_1 + (\ell\Phi_x - m\Phi_y)K_2. \tag{3.14}$$

The relationship between old and new variables is

$$\Psi_1 = \ell\Phi_x + m\Phi_z - k\theta, \qquad \Psi_2 = \ell_x - m\Phi_z,$$

$$I_x = \ell(K_1 + K_2), \qquad I_y = m(K_1 - K_2). \tag{3.15}$$

The new Hamiltonian becomes

$$H_2 = (\ell\nu_x + m\nu_y - k)K_1 + (\ell\nu_x - m\nu_y)K_2 + V_{00}(K_1, K_2) +$$

$$+ V_{00}(K_1, K_2) + V_{\ell m}(K_1, K_2)\cos\Psi_1. \tag{3.16}$$

Since this Hamiltonian is independent of θ, it is a constant of motion. In addition, it is independent of Ψ_2. Therefore,

the new action

$$K_2 = \frac{I_x}{\ell} - \frac{I_y}{m} \tag{3.17}$$

is also an invariant.

As a result the second term in (3.16) may be ignored since it just represents a constant energy term.

$$H_2 = (\ell\nu_x + m\nu_y - k)K_1 + V_{00}(K_1, K_2) + V_{\ell m}(K_1, K_2)\cos\Psi_1. \tag{3.18}$$

Suppose we define K_r as that action which yields the oscillation frequencies at resonance

$$\ell\nu_x + m\nu_y + \left.\frac{dV_{00}}{dK_1}\right|_{K_1 = K_r} = k. \tag{3.19}$$

After expansion of V_{00} close to K_r we get from (3.18) and (3.19)

$$H_2 \approx (\ell\nu_x + m\nu_y - k)K_r + \frac{1}{2}\frac{dV_{00}^2}{dK_1^2}(K_1 - K_r)^2 + V_{\ell m}(K_r, K_2)\cos\Psi_1. \tag{3.20}$$

Here we can omit once again the first term, which is now the constant energy term. Applying the third transformation with generation function

$$F_3 = (K_1 - K_r)\,\Psi_1, \tag{3.21}$$

we finally come to the pendulum like Hamiltonian

$$H_3 = \alpha\frac{p^2}{2} + V_{\ell m}\cos\Psi_1, \tag{3.22}$$

where nonlinearity α is

$$\alpha = \frac{d^2 V_{00}}{dK_1^2} = m^2 \frac{\partial \Delta\nu_y}{\partial I_y} + 2m\ell \frac{\partial \Delta\nu_y}{\partial I_x} + \ell^2 \frac{\partial \Delta\upsilon_x}{\partial I_x}. \qquad (3.23)$$

The phase space diagram for a pendulum is shown in Fig. 6. This plot was reproduced from Ref. 8.

Because the energy of pendulum is constant, the resonance width, which is equivalent to the size of the separatrix, can be easily found. It is

$$\Delta p = 4 \sqrt{\frac{V_{\ell m}}{\alpha}}. \qquad (3.24)$$

We shall consider below the flat beam case and will use the beam-beam forces in the same form as in (1.14) (See, also Ref. 9)

$$f_x = 4\pi \sqrt{2}\, F_D\,(x/\sqrt{2}),$$
$$f_y = (2\pi)^{3/2}\, e^{-x^2/2}\, \Phi\,(y/\sqrt{2}). \qquad (3.25)$$

One can get after substitution of (3.25) in (3.13)

$$\Delta\nu_x(A_x,A_y) = \xi_x \frac{\sqrt{2}}{\pi} \int_0^{2\pi} F_D(A_x \cos\Phi_x/\sqrt{2}) \cos\Phi_x d\Phi_x, \qquad (3.26)$$

$$\Delta\nu_y(A_x,A_y) = \xi_y I_0\left(\frac{A_x^2}{4}\right)\left[I_0\left(\frac{A_y^2}{4}\right) + I_1\left(\frac{A_y^2}{4}\right)\right] \exp\left\{-\frac{A_x^2+A_y^2}{4}\right\}, \qquad (3.27)$$

where I_0 and I_1 are modified Bessel functions of zero and first orders.

The example of the tune spread (beam footprint) corresponding to the equations (3.26), (3.27) is shown in

Fig. 7A. This footprint placed in the tune plane amongst the resonances is shown in the Fig. 7B. (These figures are taken from Ref. 10).

We can see from Fig. 7B that the resonance lines inside the footprint are satisfied by different amplitude conditions. It means that the resonances can equally be presented by the certain lines in the amplitude plane. Their location within the amplitude space is determined by the resonant condition (3.19):

$$\ell[\nu_x + \Delta\nu_x(A_x, A_y)] + m\,[\nu_y + \Delta\nu_y(A_x, A_y)] = k, \qquad (3.28)$$

where $\Delta\nu_x$ and $\Delta\nu_y$ are taken from (3.26) and (3.27).

An example of the resonance in the amplitude plane is shown in Fig. 8. The resonance width here is measured by the value of the maximal beating of the amplitudes, which goes in the direction determined by the invariant (3.17).

In terms of amplitudes A_x, A_y the nonlinearity α from the equation (3.23) is presented in the form

$$\alpha = \frac{m\,\beta_y^2}{A_y \sigma_y^2}\left\{\frac{\partial \Delta\nu_y}{\partial A_y} + \frac{A_y}{A_x}\frac{\xi_x}{\xi_y}\frac{\sigma_y}{\sigma_x}\left[\frac{2\ell}{m}\frac{\partial \Delta\nu_x}{\partial A_x} + \frac{\ell^2}{m^2}\frac{\partial \Delta y_z}{\partial A_x}\right]\right\}. \qquad (3.29)$$

In the case of very flat beam and in the region of moderate amplitude of vertical oscillation the first term in (3.20) is dominant. Therefore in light of (3.27) one can get

$$\alpha = \xi_y \frac{m^2 \beta_y}{A_y^2 \sigma_y^2} \exp\left(-\frac{A_x^2 + A_y^2}{4}\right) I_0\left(\frac{A_x^2}{4}\right) I_1\left(\frac{A_y^2}{4}\right). \qquad (3.30)$$

We can also rewrite equation (3.9) for $m \neq 0$ in the form

$$V_{\ell m} = \frac{\xi_y \sigma_y^2 A_y}{m\beta_y (2\sigma)^2} \int_0^{2\pi}\int f_y \cos \ell\Phi_x \sin m\Phi_y \sin \Phi_y \, d\Phi_x d\Phi_y . \qquad (3.31)$$

The integrals in (3.31) can be evaluated for f_y taken in the form (3.25). The substitution (3.31) and (3.30) into (3.24) gives for resonance width [11]

$$\Delta A_y = 2\sqrt{G_\ell(A_x)\, F_m(A_y)}, \qquad (3.32)$$

with the functions $G_\ell(A_x)$ and $F_m(A_y)$ determined as

$$G_\ell(A_x) = \frac{I_{\ell/2}\left(\frac{A_x^2}{4}\right)}{I_0\left(\frac{A_x^2}{4}\right)}, \qquad (3.33)$$

$$F_m(A_y) = \frac{2A_y^2}{m^2-1} \frac{I_{\frac{m}{2}-1}\left(\frac{A_y^2}{4}\right) + \left(1 - \frac{2(m-1)}{A_y^2}\right) I_{\frac{m}{2}}\left(\frac{A_y^2}{4}\right)}{I_1\left(\frac{A_y^2}{4}\right)} . \qquad (3.34)$$

Note, that ΔA_y do not depend on ξ_y.

The consideration above is valid for $\Delta p \ll K_r$ or for not too small nonlinearity α. Another important approximation is the approximation of single isolated resonance.

4. CHIRICOV OVERLAP CRITERION

In the reality the set of resonances turns out to be everywhere very dense. See, for example, Fig. 9, reproduced from Ref 12.

It turns out that a fairly general mechanism for arising instability of the motions is the so-called overlap of nonlinear resonances [7]. This instability has a rather peculiar nature resulting in an irregular, or stochastic, motion of the system. A plausible condition for the occurrence of the stochasticity seems to be the approach of the resonances down to the distance of the order of a resonance size. To be precise, the overlap of resonances begins when their separatrices touch each other. How to calculate the condition of separatrix touching taking into account a deformation of the separatrix by a neighboring resonance? The simplest method, suggested by Chirikov, is to consider each of the resonances as if another one were absent. It is just what one means when talking about the overlap criterion. Being a quite rough one, this criterion is fairly efficient especially in the case of rather complicated systems.

According to the overlap criterion to avoid the chaotic behavior in the simple one dimensional case one need to have

$$\delta\nu \ll \nu_1 - \nu_2, \qquad (4.1)$$

where $\delta\nu$ is the resonance width in the tune plane, calculated as

$$\delta\nu = \alpha\Delta p = 4\sqrt{\alpha \cdot V_{\ell m}} \qquad (4.2)$$

and ν_1, ν_2 are the frequencies of two neighboring resonances

$$\nu_1 = \frac{n}{m} ; \qquad \nu_2 = \frac{n'}{m'} , \tag{4.3}$$

with $nm' - n'm = \pm 1$.

Using (4.2) and (4.3) we can rewrite (4.1) in the form

$$\sqrt{\alpha V_{\ell m}} << \frac{1}{4mm'} . \tag{4.4}$$

Equation (4.4) sets a limit to the validity of the isolated resonance analysis. This condition requires that nonlinearity α not be too large since in this case the resonances do not separate.

The application of the Chirikov overlap criterion is very convenient for a numerical study of the beam-beam effects. Using the computer it is easy to observe the modifications of the phase space particle trajectory when the parameter ξ is increased and to check a moment, when the isolated separatrices become touch each other and a regular motion is destroyed. The examples of the phase space with the regular and irregular motion for one dimensional case are shown in Fig. 10. These examples were reproduced from Ref. 13.

The overlap criterion has been applied by several authors to the determination of critical value ξ_{cr} (See Ref. 13-15). In the Fig. 11 ξ_{cr} is shown in the dependence of the fraction part of the betatron tune. These calculations were done for one dimensional beam-beam model.

The resulting data is much too high compared with real experimental observations.

5. ADDING LONGITUDINAL MOTION

Including the synchrotron oscillations into the consideration will bring to the new effects. We will show that the interaction of the particle with the opposing bunch produces a coupling between synchrotron and betatron oscillations. This coupling drives the multiplets of synchrobetatron sideband resonances near the primary beam-beam resonances. There are three regimes which can characterize the resonance system now [16]. (See Fig.12). In the first regime new resonances are still isolated and do not overlap. In the second regime the distance between neighboring resonances is smaller and they overlap. Strong instability arises here, when the overlap distance extends to the distance between primary betatron resonances. In the third regime all resonances of the multiplet merge together.

It is clear that the overlap of the synchrobetatron resonances can decrease the value of the beam-beam limit.

There are several beam-beam longitudinal-transverse coupling mechanisms. We begin to consider them from the so-called **force modulation**. Such a modulation arises due to the variations of the β-function at the interaction, which are dependent from the synchrotron motion. There are two of them. They are β-function dependence from the longitudinal deviation

$$\beta_y(z) = \beta_{y0} + \frac{z^2}{\beta_{y0}} \tag{5.1}$$

and from the energy deviation $\Delta E/E$:

$$\beta_y\left(\frac{\Delta E}{E}\right) = \beta_{y0} + \frac{d\beta_{y0}}{d\left(\frac{\Delta E}{E}\right)} \cdot \frac{\Delta E}{E}, \qquad (5.2)$$

where β_{y0} is the β-function at the IP and $d\beta_{y0}/d(\Delta E/E)$ is the lattice dependent term.

Here, we will concern ourselves with the flat beam case. The round beam case will be considered in the next section. For a flat beam all modulation effects are much more significant in vertical direction.

In principle, second term in (5.2) can be made negligible by a proper choice of a chromatic correction scheme in the storage rings. Therefore, we shall not include it in the consideration below.

The longitudinal motion of a particle within the weak beam will be assumed to have the following properties. It undergoes linear synchrotron oscillations with the synchrotron tune, ν_s:

$$s = S_0 \cos \nu_s \theta. \qquad (5.3)$$

The longitudinal beam-beam impulse is assumed negligible; the direct effect of the RF cavity system on the motion of the particle is not considered. We shall also assume for a moment, that the opposing bunch has no longitudinal extent. Therefore if a particle within the weak bunch has a longitudinal offset s from the synchronous particle, it receives its transverse beam-beam kick at a distance $z=-s/2$ from the IP.

The equation (5.1) leads to ξ_y dependence from the longitudinal coordinate of the particles

$$\xi_y = \xi_{y0}\left(1 + \frac{s^2}{4\beta_{y0}^2}\right)^{1/2}. \qquad (5.4)$$

After substitution (5.3) in (5.4) we get

$$\xi_y = \xi_{y0}\left[1 + \left(\frac{\sigma_z}{2\beta_{y0}}\right)^2 A_z^2 \cos^2 \nu_s \theta\right]^{1/2}, \qquad (5.5)$$

where $A_z = S_0/\sigma_z$ is the amplitude of the longitudinal synchrotron oscillations, normalized on the bunchlength σ_z. For small A_z and $\sigma_z \sim \beta_{y0}$ we can write

$$\xi_y \simeq \xi_{y0}\left[1 + \frac{A_z^2}{4}\left(\frac{\sigma_z}{2\beta_{y0}}\right)^2 (1 + \cos 2\nu_s \theta)\right]. \qquad (5.6)$$

This means an existence of two sideband resonances

$$m\nu_y \pm 2\nu_s = k. \qquad (5.7)$$

In the case of the large longitudinal oscillations a number of the dangerous resonances is increased and we will have the following resonance conditions:

$$m\nu_y + n\nu_s = k, \qquad (5.8)$$

where m and n are even.

The force modulation results also in the tune shift dependence from the longitudinal oscillation. It directly follows after substitution (5.5) in the equation (3.13). This effect leads to the dependence of instantaneous

betatron tune on the parameters of longitudinal motion:

$$\nu_y \simeq \nu_{y0} + \Delta\nu_{y0} \left[1 + \left(\frac{\sigma_z}{2\beta_{y0}} \right)^2 A_z^2 \cos^2 \nu_s \theta \right]^{1/2}. \qquad (5.9)$$

It also drive the synchrobetatron resonances (5.8) [17].

The result of the numerical simulation of the effect of force modulation is shown on Fig. 13. It presents a significant dependence of ξ_{cr} on the amplitude of synchrotron oscillations.

Another source of the longitudinal-transverse coupling in beam-beam interaction is so-called **betatron tune modulation** [18]. This type of modulation arises due to the particle longitudinal oscillations, but attached importance of this modulation is connected with the low β-function at the IP and large accompanying betatron phase advance nearby it:

$$\Delta\Phi = \int_0^{S/2} \frac{dz}{\beta_y(z)}. \qquad (5.10)$$

While the instantaneous betatron frequency is

$$\nu_y = \nu_{y0} - \nu_s \frac{S_0}{2\beta_y} \sin \nu_s \theta, \qquad (5.11)$$

we can write for a canonical phase Φ in the Hamiltonian (3.10)

$$\Phi_y = \int_0^{\theta} \nu \, d\theta = \nu_{y0}\theta + \frac{S_0}{2\beta_y} \cos \nu_s \theta. \qquad (5.12)$$

The substitution of (5.12) in (3.10) yields new resonance conditions

$$\ell\nu_x + m\nu_y + n\nu_s = k, \qquad (5.13)$$

with ℓ, m, n being even numbers and new resonance harmonic amplitude

$$V_{\ell mn} = V_{\ell m} J_n \left[m \left(\frac{\sigma_z}{2\beta_y} \right) A_z \right], \qquad (5.14)$$

where J_n is the Bessel function of the order n.

It was shown in the recent studies [19], that for relatively small amplitudes of the longitudinal oscillations the consideration of the finite longitudinal extent of the bunch results with an additional reduction factor

$$Y = \exp \left\{ -\frac{1}{2} \left(\frac{m\sigma_z}{2\beta_y} \right)^2 \right\}, \qquad (5.15)$$

in the resonance harmonic amplitude $V_{\ell mn}$. It is connected with the effect of the beam-beam kick averaging in the betatron phases and with the reduction of the kick strength.

Two things contribute to the reduction of the beam-beam kick [10]. The deflection experienced by the particle during the interaction with the opposing bunch is proportional to the average charge density of the opposing beam over the length of interaction. Therefore, due to the β-function variation nearby the IP the deflection produced by the integrated kick is less than the impulse - like kick at the symmetry point where β-function is at a minimum. Next is for

particles with small displacements. As the particle trajectory places it closer to the center of the opposing beam core it experiences less beam-beam force. Summed over the length of the interaction the net deflection is less. Fig. 14 shows the result of calculation of particle trajectory for both the impulse - like and integrated kick cases.

Numerical studies of the tune modulation effect on the critical value ξ_{cr} usually show the significant reduction of ξ_{cr}, when the depth of the modulation is increased. In Fig. 15 such an example, taken from the Ref. 17, is shown.

Non-zero chromaticity is also the source of tune modulation. But it is usually compensated to a very small value.

In principle, the dependence of the rotation period on a particle energy leads also to the excitation of the synchrobetatron resonances. But this source of the effect is a very weak.

The next source of longitudinal - transverse coupling in beam-beam interaction - non-zero dispersion at the IP - will be considered in the separate section.

6. COLLISION OF ROUND BEAMS

An idea of a collision of the round e^+e^- beams has been circulated since early storage rings. Also nowadays it has been studied intensively and considered as a very promising

attempt in the advance towards to high luminosity. What is so attractive in the round beams?

First is the factor of two in luminosity, which directly follows from the luminosity formula (2.9) at $\sigma_y = \sigma_x$ with all other parameters being the same as for flat beams.

Second is the absolute elimination of the force modulation effect, when $\beta_x \equiv \beta_y$. It follows from the independence of ξ from the beta-function in the round beam case

$$\xi = \frac{Nr_e}{4\pi\gamma\varepsilon}, \qquad (6.1)$$

where ε is the beam transverse emittance.

Third is the reduction of the beam-beam problem from three to two dimensions of freedom. Equal vertical and horizontal emittances and betatron tunes are implicit initial conditions here.

The simulation of the beam-beam effects in the round beam configuration in a 'weak - strong' case with the finite bunch length taken into account was carried out by several authors. The typical result consists in a rather big maximal value of ξ, determined by a threshold in a beam core blow up. See, for example, Fig. 16 reproduced from Ref. 20.

However, the maximal ξ for a particles with large longitudinal excursions from a bunch center is substantially lower. The deterioration is connected with the effect of tune modulation, considered above. For a large amplitude of longitudinal oscillations, a strong longitudinal-transverse coupling appears that results in a fast loss of these

particles on the aperture. The maximal attainable value of ξ in the dependence of a given longitudinal amplitude is shown in the Fig. 17 [20].

We should mention here, that the realization of the low beta function in both directions as low as in the flat beam design will demand approximately two times stronger sextuple lenses for a chromaticity correction. This fact reduces the attraction of the round beam concept if one takes into account the possible effects that can arise due to the interference of the beam-beam effects and machine imperfections.

7. NON-ZERO DISPERSION AT THE INTERACTION POINT

For a long time among the accelerator physicists there is a firm prejudice against the dispersion at the interaction point. It is confirmed by experimental observations and by simulations as well.

All these studies were carried out when the contributions of the energy and betatron oscillations to the total transverse beam dimension in the dispersive direction were comparable, i. e. the magnitude

$$\lambda = \frac{\sigma_{xs}}{\sigma_{x\beta}}, \qquad (7.1)$$

(where $\sigma_{x\beta}$ is the betatron beam size, $\sigma_{xs} = |\Psi|\ \sigma_{\varepsilon}$ is the synchrotron beam size, Ψ is the dispersion at the IP and σ_{ε}

is the beam energy spread) satisfied the condition

$$\lambda \lesssim 1. \qquad (7.2)$$

The adopted conclusion is as follows. The dispersion at the IP causes the excitation of the synchrobetatron resonances

$$\ell\nu_x + m\nu_y + n\nu_s = k, \qquad (7.3)$$

with m and $(\ell + n)$ being even numbers and results in the deterioration of the maximal ξ.

What happens, if one makes

$$\lambda \gg 1. \qquad (7.4)$$

Is the deterioration process continuing?

To answer that question, the analysis of this case was carried out in Ref. 21. A method for a creation of a big λ was assumed, where not only a big dispersion at the IP was used, but a low beta function and very small emittances as well. This approach results in a very flat beam configuration at the IP

$$\frac{\sigma_x}{\sigma_y} \geq 250 \qquad (7.5)$$

and a large difference between ξ_y and ξ_x

$$\frac{\xi_y}{\xi_x} \geq 5. \qquad (7.6)$$

For the case of $\lambda \gg 1$ the particle excursion from the center in horizontal direction is

$$X = \frac{A_x}{\lambda} \cos\vartheta_x + A_s \cos\vartheta_s, \qquad (7.7)$$

where X is the coordinate normalized on the total beam size $\sigma_x = \sqrt{\sigma_{x\beta}^2 + \sigma_{xs}^2}$ and A_s is the synchrotron amplitude, normalized by a condition

$$A_s = \frac{|\Psi|\ \Delta E/E}{\sigma_{xs}}, \qquad (7.8)$$

where $\frac{\Delta E}{E}$ is the energy deviation.

It was estimated in Ref. 21, how the width of the resonances (7.3) depends on the parameter λ. We can do this in a similar fashion to two dimensional case, considered in the section 3. Therefore, according to the equation (3.31) the resonance harmonic amplitude $V_{\ell mn}$ is

$$V_{\ell mn} = \frac{\xi_y\ A_y\ \sigma_y^{\ 2}}{(2\pi)^{\ 3} m\ \beta_y} \int_0^{2\pi}\!\!\int\!\!\int d\vartheta_x \cdot d\vartheta_y \cdot d\vartheta_s \times$$

$$f_y\left(\frac{A_x}{\lambda}\cos\vartheta_x + A_s\cos\vartheta_s,\ A_y\cos\vartheta_y\right)\times$$

$$\cos\ell\vartheta_x \cdot \cos n\vartheta_s \cdot \sin\vartheta_y \cdot \sin m\vartheta_y. \qquad (7.9)$$

Here $m \neq 0$.

Nonlinearity α has the same expression as in (3.10) with the substitution A_s instead of A_x.

It is natural to use f_y in (7.9) in the flat beam presentation of (3.25). It allows to factorize the evaluation of the integrals in (7.9), that results in an expression analogous to (3.32) for the width of any particular resonance with the numbers ℓ, m, n:

$$\Delta A_y = 2\sqrt{G_{\ell n}(A_x, A_s)\ F_m(A_y)}. \qquad (7.10)$$

Here the functions, F_m, have exactly the same form as in (3.34), but the functions $G_{\ell n}$ are different than in (3.33). They can be found for every ℓ after expansion of f_y in a Taylor series of a small term A_x/λ. Several results of the evaluation of leading terms in $G_{\ell n}$ are presented below.

For $\ell = 0$

$$G_{on}(A_s) = \frac{I_{n/2}\left(\frac{A_s^2}{4}\right)}{I_0\left(\frac{A_s^2}{4}\right)}, \qquad (7.11)$$

where $I_{n/2}$ is the modified Bessel function of the order $n/2$.

For $\ell = 1$ the leading term of $G_{\ell n}$ already contains a small factor $A_x/2\lambda$:

$$G_{1n} = \frac{A_x \cdot A_s}{4\lambda} \frac{I_{(n-1)/2}\left(\frac{A_s^2}{4}\right) - I_{(n+1)/2}\left(\frac{A_s^2}{4}\right)}{I_0\left(\frac{A_s^2}{4}\right)}, \qquad (7.12)$$

For $l=2$

$$G_{2n} = \frac{1}{2}\left(\frac{A_x}{2\lambda}\right)^2 \times$$

$$\frac{I_{n/2}\left(\frac{A_s^2}{4}\right)\left(\frac{A_s^2}{2}-1\right)+\frac{A_s^2}{2}\left[I_{n/2-1}\left(\frac{A_s^2}{4}\right)+I_{n/2+1}\left(\frac{A_s^2}{4}\right)\right]}{I_0\left(\frac{A_s^2}{4}\right)} \quad (7.13)$$

and for higher orders of ℓ we have

$$G_{\ell n} \sim (A_x/2\lambda)^{\ell}. \quad (7.14)$$

Thus, we come to the following conclusion. The width of the pure vertical resonances does not depend on the parameter λ. The width of all other resonances is reduced with the increasing parameter λ. The expected effect is estimated as follows:

$$\Delta A_y \sim (2\lambda)^{-\ell/2} \quad (7.15)$$

To clarify the importance of this effect for beam-beam interactions in the situation when the total number of the resonances is increased by the new set of the synchrobetatron satellites, we have accomplished the following program of the analytical and numerical study of the beam-beam effects. In the beginning we found the dependence of the blow-up effect of the 'weak' beam on the working point on the tune plane. Then, in two good working points we calculated the dependence of this effect on the intensity of the 'strong' beam.

For a fast analysis of a large number of betatron tunes a simple one dimensional analytical model ($\xi_x = 0$) has been

proposed for determination of blown up σ_y. The model is based on the crude approximation for the relaxed distribution function of the particle density, where the particle density within the nonlinear resonance is supposed to be constant.

The validity of the model was checked by the conventional tracking technique. In Fig. 18 the results of the model prediction are presented with the solid lines and the tracking results are presented with crosses. Here, the ratio σ_y/σ_{y0}, where σ_{y0} is the vertical size of the "strong" beam, is shown in the dependence on ν_y at a fixed horizontal betatron tune $\nu_x = 0.08$. Other parameters were chosen as $\nu_s = 0.025$, $\xi_y = 0.05$, $\xi_x = 0.01$ and $\lambda = 5$.

We found the analytical result in a satisfactory agreement with simulations. Then, the model calculations of the vertical beam size were extended on the whole tune plane. For given values $\xi_y = 0.05$ and $\nu_s = 0.025$ and for four values of λ (λ=2.5, λ=5, λ=10 and λ=25) we determined σ_y/σ_{y0} in every point of the betatron tune on the mesh with the step $\Delta\nu_x = \Delta\nu_y = 0.005$. As a result we get the areas of tunes where the blow-up of σ_{y0} did not exceed 15%. In Fig.19 these areas are contoured and marked with shading for each value of λ. In every plot all resonances up to six order are also shown.

Our conclusion based on the analysis of these four cases is as follows. Most destructive resonances are pure vertical betatron and synchrobetatron resonances with the numbers

$|m|=0$, 2, 4, 6 and $|n|=0,2$. The effect of these resonances is observed independent of the parameter λ in all four plots. At the same time all pure horizontal and coupling resonances are sensitive to the parameter λ. Their relative importance depends on the number ℓ. For example at $\lambda = 5$ the resonances $\pm 3\nu_x + 2\nu_y \pm \nu_s = 1$ with $\ell = 3$ are looked as the resonances limiting the good areas. At the same time they are less important at $\lambda = 10$, where the limiting resonances are the resonances $\pm 2\nu_x + 2\nu_y = 1$ and $\pm 2\nu_x + 2\nu_y \pm 2\nu_s = 1$ with $\ell=2$. Correspondingly, the good areas are increased here compared to the previous case. The largest areas are on the plot with $\lambda=25$. Here only the resonances $\pm 2\nu_x + 4\nu_y = 1$ and $\pm \nu_x + 2\nu_y \pm \nu_s = 1$ are considered as the destructive resonances.

The dependence of the 'weak' beam vertical size on the linear tune shifts ξ_y, ξ_x has been studied numerically at a constant synchrotron tune $\nu_s = 0.025$ for two working points with the betatron tunes ($\nu_x = 13.08$, $\nu_y = 7.075$) and ($\nu_s = 13.08$, $\nu_y = 7.10$). According to the plots in Fig. 19 we considered these working points very promising for the case of the big parameter λ.

Numerical simulations were done in the model including longitudinal motion, quantum fluctuation noise and radiation damping with the damping time expressed in the numbers of beam-beam collisions $N=9090$ for longitudinal and vertical oscillations and $N=4545$ for horizontal oscillations. There were four sets of calculations in each working point. One for zero dispersion ($\lambda=0$), one for small dispersion ($\lambda=0.7$)

and two for the big dispersion ($\lambda=5$ and $\lambda=25$). The results are presented in Fig. 20. They give a clear evidence of the effectiveness of a big dispersion in the suppression of the resonance $2\nu_x - 2\nu_y = k$ and its synchrobetatron satellites. In our simulation we had the longitudinal beam size $\sigma_z = 0.75$ cm, while the vertical beta function at the IP was 1 cm.

8. COLLISION WITH CROSSING ANGLE

An idea to use the crossed beams in e^+e^- storage rings has a long history. The main motivation here is the achievement of the fast separation of the colliding beam orbits. It allows an increase in collision frequency (number of bunches) and avoids beam-beam interactions in the parasitic crossings.

Unfortunately, this method is not free from the problem shown in Fig. 21. (See also Ref. 22). The particle with a distance s from the center of its own bunch passes the center of the opposing bunch at a transverse position $x + s\varphi$, where x is the transverse displacement of a particle inside the bunch and φ is a half of the crossing angle.

Thus, due to the crossing angle we get the modulation of the transverse particle coordinate with synchrotron oscillations like in the case of non-zero dispersion at the IP considered in previous section. The value of the effective dispersion, Ψ_{eff}, is

$$\frac{\Psi_{eff}}{\Psi} \lesssim 1, \qquad (8.4)$$

or

$$\varphi \simeq \nu_s \frac{\Psi}{\alpha R} . \qquad (8.5)$$

In terms of the parameter λ the equality Ψ_{eff} and Ψ gives an addition improving factor of $\sqrt{2}$

$$\lambda = \frac{|\Psi + \Psi_{eff}|\sigma_\varepsilon}{\sigma_{x\beta}} \simeq \sqrt{2}\ \lambda_0, \qquad (8.6)$$

where λ_0 is the value of the parameter λ without crossing angle. Thus, the crossing angle in the second case does not lead to new phenomena and moreover leads to better conditions in the beam-beam interaction. As a result, we can suspect that the summary effect of a big dispersion and the collision at a crossing angle will open a new way towards the high luminosity.

To be accurate, we should say that the synchrotron oscillation is also influenced by the betatron one. The energy shift $\delta E/E$ after the interaction is

$$\frac{\delta E}{E} = \phi\ \Delta x' . \qquad (8.7)$$

Howener, due to the big difference in the longitudinal and transverse emittances it does not results in any destructive effects.

9. INTERFERENCE OF THE BEAM-BEAM EFFECTS AND MACHINE IMPERFECTIONS

We shall consider below several types of machine imperfections that can cause a reduction of the maximal ξ.

The first is nonlinear components of the guiding magnetic field. We imply here the sextuple and octupole lenses and additional uncontrolled cubic and high order machine nonlinearities. We know that, even in the single beam case, they may reduce the aperture from the free mechanical aperture to the so-called dynamic aperture. In the two beam case with beam-beam effects a small size of the dynamic aperture might be a cause of ξ limitation. This was observed on VEPP-2M storage ring [23], where the dependence of the ultimate ξ_y value on the position of the aperture scraper was studied. The result is shown in the Fig. 22. It is seen that the ξ_y is independent of the scraper position above the aperture of $35\sigma_y$. Below this aperture ξ_y is decreasing. The existence of the threshold is a clear evidence for dynamic aperture limit at $35\sigma_y$.

Recently, it was noticed on the example on cubic nonlinearity [24], that even in the case when the betatron tunes are chosen far from the destructive machine resonances, the zero harmonic of the nonlinearity can lead to significant effects. A dangerous situation arises at the oscillation amplitudes where beam-beam detuning is partly or totally compensated by a cubic machine nonlinearity. This

means that the resonance self stabilization is absent here and the resonance width can extend to the large amplitudes. The same follows from the formula (3.24) for resonance width. At constant harmonic amplitude, the resonance width can be sufficiently increased by diminishing of the nonlinearity α.

According to the conventional notation we shall define the average cubic machine nonlinearity as

$$R_x = \frac{1}{\varepsilon_x}\frac{d\nu_x}{dA_x^2}, \qquad R_y = \frac{1}{\varepsilon_y}\frac{d\nu_y}{dA_y^2}, \tag{9.1}$$

where ε_x, ε_y are horizontal and vertical beam emittances and A_x, A_y are normalized betatron amplitudes. These nonlinearities contribute to the Hamiltonian (3.10) with the term [24]

$$W_{00} = R_x I_x^2 + R_y I_y^2 - 4\sqrt{R_x R_y}\, I_x I_y. \tag{9.2}$$

Now, all formulae of the section 3 are valid after substitution

$$V_{00} + W_{00} \rightarrow V_{00}. \tag{9.3}$$

Therefore, it is not surprisingly that the positions of the resonance lines in the amplitude plane are changed and, at certain conditions, the new nonlinearity α can be very small.

The effect of the cubic machine nonlinearity on the example of resonance $10\nu_y=96$ was studied numerically in Ref.11. Three cases with zero, positive and negative nonlinearity are shown in the Fig. 23. All three were

calculated at $\nu_y=9.599$, $\nu_x=8.555$, $\xi_y=0.03$, $\xi_x=0.01$. The magnitude of the machine induced tune shifts were $\Delta\nu_x=\pm 2.5\cdot 10^{-5}$ at $A_y=0$, $A_x=1$ and $\Delta\nu_y=\pm 2.5\cdot 10^{-7}$ at $A_y=1$, $A_x=0$.

In all three cases the direction of resonant oscillations is vertical. In the case (*a*) the resonance spans the amplitudes $A_y=20$-40 at $A_x=0$. However, the aperture is at about 80, and without additional resonances, it is very difficult for a particle to over come the very strong damping between 40 and 80. The situation changes dramatically when positive nonlinearity is added (case *b*). In a certain region in amplitude space the beam-beam induced nonlinearity is canceled by the machine nonlinearity and a region of very wide oscillations appears. At $A_x = 1.5$ the resonance spans the entire distance from $A_y = 15$ to $A_y = 70$. In this case a lower edge of the resonance can be considered as nonlinear dynamic aperture.

In the third case, when machine nonlinearity is negative, such region is absent and the machine nonlinearity is simply bending the resonance upwards as A_x increases.

An experimental observation of the machine nonlinearity influence on the resonances, induced by beam-beam effects, was done on VEPP-4 storage ring [25]. The methods applied was the observation of the particle loss rate during the betatron tune scan. An example of such observation is shown in the Fig. 24. All regions with the high particle loss rate are easy identified with the certain resonances.

There were several scans across the resonance $7\nu_x=60$

with different values of the cubic nonlinearity. The results of two of them with $R_x \simeq \pm 6.9$ cm^{-1} are shown in the Fig. 25. It is interesting to mention that the specific luminosity, $L_{Sp} = L/i^+i^-$, does not change, while the loss rate is changed significantly.

A second example of a machine imperfection is a small ($\lesssim 0.1\sigma_{x,y}$) separation of the colliding beam orbits. This effect is especially important for two ring colliding beam facilities. The orbit separation breaks the symmetry of the beam-beam interaction potential, that results in the appearance of the odd resonances in addition to the even resonances. The set of even and odd resonances can overlap much easier than the set of only even resonances.

The appearance of the odd resonances at a small orbit separation was observed on VEPP-4 storage ring [25]. Fig.26*a* presents the diagrams of the loss rate and specific luminosity during the scans across the resonance $7\nu_x = 60$ at a different orbit separations. At a zero separation (Fig. 26*b*) the resonance $7\nu_x = 60$ disappears, while the resonance $14\nu_x = 120$ is not observed.

It is interesting to note that the loss rate observation on the 'anomalous' high order beam-beam resonances looks much more effective for an accurate tuning of beam collisions than the observation of the specific luminosity.

In practice, a static orbit separation can be accomplished by the orbit separation ripple, which is only worsening a common situation.

A third source of the machine effect on the beam-beam interaction is the asymmetry in the betatron phase advance, $\mu_{x,y}$, between interaction points, that also leads to the appearance of the additional 'anomalous' resonances. Two effects were observed on the VEPP-2M storage ring [26] with the variation of phase advance of the vertical betatron oscillations, $\Delta\mu_y$. They are the blow up of the vertical beam size (see Fig. 27*a*) and the degradation of the maximal ξ_y (see Fig. 27*b*).

10. STRONG-STRONG INTERACTION AND FLIP-FLOP EFFECT

A consideration of the beam-beam effects in the 'weak-strong' approximation is capable to give us the understanding of the phenomena leading to the beam intensity limitation. At the same time, such a consideration can hardly pretend to make an exact prediction of the limit value in the real life, where we already deal with two beams with almost equal intensity. This is clearly demonstrated by the observation, performed on VEPP-2M storage ring [26]. In the Fig. 28 one can find a big difference between 'weak-strong' and 'strong-strong' cases in the vertical beam size behavior versus the strong beam intensity.

It means that an ideal solution of the beam-beam problem must be self-consistent. Such an attempt has been made in Ref.27 for a phenological explanation of the flip-flop

effect. Similar studies were carried out in Ref.28 and Ref.29.

A flip-flop effect occurs between the sizes of the two beams. It was observed that with the increased intensity of both beams one beam gains dominance over the other, blowing it up while reducing its own size. The collapsed beam effectively becomes stronger, while the blown-up beam effectively becomes weaker. Reversing the roles of the beams is possible by exerting some asymmetric external influence.

The following system of algebraic equations for a description of the internal links between the beam dimensions and currents was proposed in Ref. 27:

$$\begin{cases} \sigma_+^2 = \sigma_0^2 + \left(\dfrac{a\,i^-}{\sigma_-}\right)^p \\ \sigma_-^2 = \sigma_0^2 + \left(\dfrac{a\,i^+}{\sigma_+}\right)^p \end{cases} . \qquad (10.1)$$

Here σ_0 is the natural size, supposed to be the same for both beams; σ_+, σ_- are blown-up beam dimensions; i^+, i^- are beam currents and a, p are some unchanged parameters. The latter parameters are supposed to be determined by all know constants affecting beam size, but the nature of the effects is not figured out.

At constant currents each equation in (10.1) describes the dependence of one beam size on the opposite beam size. It is shown in the Fig. 29 for three values of i^+.

Evidently, the self-consistent solution lies on the

diagonal, where both beams have equal dimensions. There are two cases of interest, depending from the slope of the curve on the diagonal.

If

$$\frac{\partial\sigma_+}{\partial\sigma_-} > -1, \qquad (10.2)$$

than the diagonal point is a stable focus. (See Fig. 30a). But if

$$\frac{\partial\sigma_+}{\partial\sigma_-} < -1, \qquad (10.3)$$

the diagonal point becomes an unstable saddle (see Fig. 30b) and two new stable points appear (see Fig. 31). At

$$\frac{\partial\sigma_+}{\partial\sigma_-} = -1, \qquad (10.4)$$

a solution of (10.1) is changing from equal dimension beams to the flip-flop beams. This condition correspondents to a certain beam current, that we define as the critical one. At the natural assumption $i^+ = i^- = i$, that we use for a simplification, the critical current, i^*, is [27]

$$i^* = \frac{\sigma_0^{(1+2/p)}}{a}\left(\frac{p}{p-2}\right)^{1/2}\left(\frac{2}{p-2}\right)^{1/p}, \qquad (10.5)$$

and a critical size, σ^*, is

$$\sigma^* = \sigma_0\left(\frac{p}{p-2}\right)^{1/2}. \qquad (10.6)$$

It is interesting to mention here that i^* and σ^* are increased as p approaches 2. At $p = 2$, i^* and σ^* are

infinitely big, that means the absence of the flip-flop effect.

The above consideration of the flip-flop effect gave us an example where 'strong-strong' behavior of the beams can be derived from a 'weak-strong' behavior. It is very advantageous because it allows to reduce the complexities of a 'strong-strong' model of beam-beam interactions to much more easy 'weak-strong' model.

11. ADDING RADIATION DAMPING AND QUANTUM FLUCTUATION NOISE

It is a well known fact that the electrons and positrons in the storage ring undergo radiation damping accompanied by a quantum fluctuation noise. Therefore, a correct description of the beam-beam effects should use these in the model. Below we show that damping and noise in the particle motion lead to a new phenomena, which is absent in the conservative case.

We begin with the experimental observations. Collected data from various machines, concerning ξ dependence over the damping decrements, is shown in Fig. 32.

In both plots the spread at any particular decrement value is quite large and any correlations, where the maximal ξ are figured out from the decrements, look quite speculative.

The observations of the maximal ξ values, performed in

almost identical experimental conditions during the energy scan on VEPP-4, show a weak dependence of ξ from the damping decrements (see, Fig. 33).

In the last decade several theories of beam-beam effects, including noise and damping had appeared [30-32]. All of them had a goal to calculate the particle distribution in the presence of the nonlinear resonances that allows finding beam blow up and particle losses at a certain aperture. A common method is the solution of the Fokker-Planck equation for the evolution of the particle distribution. Recently, these studies were renovated and several new results were obtained [33-35]. Here, we shall review briefly main ideas of the References 33 and 34 in the application to the beam-beam effects.

The influence of the radiation damping and quantum fluctuation noise can be considered by adding to the Hamiltonian equations the dissipative and random terms:

$$\dot{X} = \frac{\partial H}{\partial P}\,,$$

$$\dot{P} = \frac{\partial H}{\partial X} - \gamma P + \sqrt{2\eta}\ \zeta\,(t), \tag{11.1}$$

where H is the Hamiltonian (3.1) γ in this section is the damping decrement and η is the diffusion coefficient. The random process $\zeta\,(t)$ is a 'white noise' process:

$$\langle \zeta_i(t)\ \zeta_j(t+\tau)\rangle = \delta_{ij}\delta(\tau) \tag{11.2}$$

and the symbol < > denotes the averaging in time.

The Fokker-Plank equation (FPE), describing the evolution of the particle distribution function, has the form [36]

$$\frac{\partial \rho}{\partial t} + \mathrm{P}\,\frac{\partial \rho}{\partial \mathrm{X}} - \omega \mathrm{X} - \frac{\partial (V \cdot \delta_{\mathrm{T}}(t))}{\partial \mathrm{X}}\,\frac{\partial \rho}{\partial \mathrm{P}} = \frac{\partial}{\partial \mathrm{P}}\left(\gamma \mathrm{P}\rho + \eta\,\frac{\partial \rho}{\partial \mathrm{P}}\right), \quad (11.3)$$

where V is a pertubation potential from the Hamiltonian (3.1).

In the absence of the perturbation Eq. (11.3) yields the stationary Hibbs distribution,

$$\rho = N \exp\left\{-\frac{\gamma}{\eta}\left[\frac{1}{2}\,(\mathrm{P}^2 + \omega_\ell^2 \mathrm{X}_\ell^2)\right]\right\}, \quad (11.4)$$

with the temperature $kT = \eta/\gamma$ and ω_ℓ being the betatron frequencies. (Summation over repeated indices is implied).

For a solution of (11.3) in the case of time dependent perturbation the following assumptions are useful: the smallness of damping and noise relative to unperturbed dynamics; the averaging of ρ in oscillation phases on the large interval of betatron oscillations; the slow variation of ρ will depend only on the action variables, ρ (J, t). The resulting, so-called, thermal-averaged FPE is

$$\frac{\partial \rho}{\partial \tau} = \frac{\partial}{\partial J_k}\left(-\gamma F_k(\mathrm{J}) + \eta G_{k\ell}(\mathrm{J})\,\frac{\partial \rho}{\partial J_\ell}\right), \quad (11.5)$$

where the quantities F_k, $G_{k\ell}$

$$F_k = -\left\langle p_i \frac{\partial J_k(\mathrm{X},\ \mathrm{P})}{\partial P_i}\right\rangle,$$

$$G_{k\ell} = \left\langle \frac{\partial J_k(\mathrm{X},\ \mathrm{P})}{\partial P_i}\,\frac{\partial J_\ell(\mathrm{X},\ \mathrm{P})}{\partial P_i}\right\rangle, \quad (11.6)$$

are the averages along the trajectories of the unperturbed Hamiltonian and time.

The relaxed distribution function RDF is the solution of the stationary form of Eq. (11.5)

$$\frac{\partial}{\partial J_k}\left(-\gamma F_k(\mathrm{J}) + \eta G_{k\ell}(\mathrm{J})\,\frac{\partial \rho}{\partial \mathrm{J}_\ell}\right) = 0. \quad (11.7)$$

The divergence form of Eq. (11.7) means the existence fluxes in phase space, which are circulated in closed loops. This process was called as phase convection.

Most interesting for us are the probabilities of large fluctuations, defined by the 'tails' of the RDF at $|\mathrm{J}| >> \eta/\gamma$. Therefore, we can apply the weak-noise asymptotic (WNA) $\eta \to 0$, corresponding to the low-temperature limit $kT \to 0$, for a description of RDF

$$\rho\ (\mathrm{J},T) = Z(\mathrm{J})\ \exp\left\{-\frac{\Phi(\mathrm{J})}{kT} + O(kT)\right\}, \quad (11.8)$$

and reduce the complexity of second order FPE for ρ to the first order equation for function Φ [37].

The influence of isolated nonlinear resonances on the RDF and the associated speed-up of the escape rate can be

best described in WNA through the concept of the extreme trajectory. This is the most probable trajectory of the particle to reach the point of the space J starting from the center J = 0.

For the initial conditions outside the separatrix (the 'tube') of Fig. 34, the trajectories of damping particles differ only little $\sim V^{1/2}$ from the unperturbed ones. For initial conditions inside the separatrix (inside the 'tube') the trajectories go by the contracting spiral along the central line of the 'tube', if the damping is small enough $\gamma << V$. This phenomenon was identified first in Ref. 38 and named 'resonance streaming'. The speed $\dot{J}_r$ of the motion along the resonance line can be found by decomposing the vector of the damping force F_0 in two components - F_ℓ, parallel to the vector of the resonance oscillations $\bar{\ell} = (\ell, m)$, and F_r, tangent to the resonance line, so that $\dot{J}_r = \gamma F_r$. Thus, neglecting the motion on the small scale of the order of the resonance width $\sim V^{1/2}$ one can say that the resonance cancels the component of the damping force F_ℓ along the direction of resonance oscillations and the particle moves along the resonance line under the influence of the component F_r.

The particle motions driven by noise and damping along narrow $\sim V^{1/2}$ resonance 'tube' can be effectively considered one-dimensional. With this additional simplification the variation of Φ along the resonance line is described by one-dimensional equation

$$F_r \frac{d\Phi}{dJ_r} + G_r \left(\frac{dF}{dJ_r}\right)^2 = 0, \qquad (11.9)$$

where J_r is the distance $|J|$ along the resonance line, while F_r and G_r are the components of damping force and diffusion taken along the resonance.

Two possible solutions of Eq. (11.9), $d\Phi/dJ_r = 0$ and $d\Phi/dJ_r = -F_r/G_r$, correspond to two possible directions of the extreme trajectories in the resonance - along and against the component F_r. It is clear that the function Φ measuring the difficulty of attaining given points of the phase space stays constant on a certain section of the extreme trajectory if this section coincides with the motion under the influence of damping. An example of this case is shown in Fig.35a. The motion against damping is 'difficult', so that the function Φ grows along the extreme trajectory ($d\phi/dJ_r \neq 0$). Nevertheless, the easiest path to some point J_0 from the center J = 0 may pass a large distances inside the resonance 'tube'. An example of this case is shown in Fig.35*b*.

Owing to the existence of the extreme paths, new attractive phase space regions other than the center J = 0 are possible and the circulated particle fluxes are formed as is shown in Fig. 36.

Similar effects were observed on VEP-1 storage ring after excitation of a single beam by an external periodically driven force [39]. See Fig. 37, where TV

representation of the beam transverse cross-section is shown. Here, new attracted regions other than the beam center are clearly observed.

Being inside the resonance 'tube' the particle may deviate from the central line and reach the separatrix surface with an exponential small probability

$$\Delta W \sim \exp\left(-\frac{\gamma B}{\eta}\right), \qquad (11.10)$$

where the quantity B is proportional to the resonance width. The weaker the resonance, the higher probability to escape.

With the technique discussed above, one can calculate the RDF for the case, when particle motion is perturbed by several isolated (non-overlapping) nonlinear resonances. The example of two dimensional calculations, performed for the regime with the betatron tunes $\nu_x = 0.025$, $\nu_y = 0.15$ and for radiation damping in numbers of beam-beam interactions $N = 3 \cdot 10^3$, is shown in Fig.38*a*. Here, the level lines of a function $\rho(A_x, A_y)/(A_x A_y)$ are presented. Each new line corresponds to the exponential reduction of the particle density with the factor e. Similar distribution of the particle density was constructed by a special tracking technique in the 'weak-strong' simulation of beam-beam interactions for the case of a big dispersion at the IP. The result of the study in the model not included the effect of tune modulation is shown in Fig. 38*b*. The coincidence of analytical and numerical results are quite satisfactory

here. But the coincidence was dropped in the fully three dimension case when the tune modulation was added to simulation (see Fig.39).

A similar tracking technique with the step-by-step determination of the level lines of particle density was developed for lifetime calculations in beam-beam interactions. Then, it was applied to an analysis of the regime with a big dispersion at the IP [21]. The cases of zero dispersion ($\lambda = 0$), moderate dispersion ($\lambda = 0.7$) and two cases of a big dispersion ($\lambda = 5$, $\lambda = 25$) were studied in two working points of the betatron tunes near the main coupling resonance. The result of this study is presented in Fig. 40.

Here, one can see that the best lifetimes are related to the big dispersion cases. This give us additional evidence for the effectiveness of a big dispersion in the suppression of all coupling resonances.

Acknowledgements. I am very grateful to my wife Lyuba for her patience and encouragements.

I also wish to thank V. Lebedev, D. Rice and D. Shatilov for reviewing the manuscript and useful suggestions.

APPENDIX:

Potential of a 3-Dimensional Gaussian Charge Distribution [1]

Consider the Poisson equation

$$\nabla^2 U(\mathbf{r}) = -4\pi\rho(\mathbf{r}), \tag{A.1}$$

with charge distribution $\rho(\mathbf{r})$, where $\mathbf{r}$ denotes $(\bar{x}, \bar{y}, \bar{z})$.

The Green's function corresponding to (A.1) has been well known in the form

$$G(\mathbf{r}, \xi) = \frac{1}{4\pi|\mathbf{r} - \xi|}, \tag{A.2}$$

which satisfies the equation

$$\nabla^2 G(\mathbf{r}, \xi) = -\delta(\mathbf{r} - \xi), \tag{A.3}$$

where ξ denotes (ξ_1, ξ_2, ξ_3). Now we rewrite the Green's function (A.2) by an integral representation

$$\frac{1}{4\pi|\mathbf{r} - \xi|} = \frac{1}{2\pi^{3/2}} \int_0^\infty \exp\left[-|\mathbf{r} - \xi|^2 q^2\right] dq, \tag{A.4}$$

which is well known as the integration formula. Note that couplings among three coordinates $(\bar{x}, \bar{y}, \bar{z})$ appearing on the left-hand side of (A.4) are separated in the integral. For later application, we make a change of the integration variable

$$t = \frac{1}{q^2}, \tag{A.5}$$

then

$$G(\mathbf{r}, \xi) = \frac{1}{4\pi^{3/2}} \int_0^\infty \frac{\exp[-|\mathbf{r} - \xi|^2/t]}{t^{3/2}} dt. \tag{A.6}$$

Using (A.6), we obtain a formal solution of the Poisson equation

$$U(\mathbf{r}) = \frac{1}{\pi^{1/2}} \int_0^\infty \frac{dt}{t^{3/2}} \iiint_{-\infty}^{\infty} d\xi \rho(\xi) \exp\left[-\frac{|\mathbf{r} - \xi|^2}{t}\right]. \tag{A.7}$$

Now, we consider a three-dimensional Gaussian charge distribution

$$\rho(\mathbf{r}) = \frac{Ne}{(2\pi)^{3/2} abc} \exp\left[-\frac{\bar{x}^2}{2a^2} - \frac{\bar{y}^2}{2b^2} - \frac{\bar{z}^2}{2c^2}\right], \tag{A.8}$$

where a, b, c are the standard deviations.

Substitution of (A.8) into (A.7) yields

$$U(\mathbf{r}) = \frac{1}{(2\pi)^{3/2} abc\pi^{1/2}} \int_0^\infty \frac{dt}{t^{3/2}} \times$$

$$\iiint_{-\infty}^{\infty} d\xi \exp\left[-\frac{|\mathbf{r} - \xi|^2}{t} - \frac{\xi_1^2}{2a^2} - \frac{\xi_2^2}{2b^2} - \frac{\xi_3^2}{2c^2}\right] \tag{A.9}$$

and one can get after integration

$$U(\mathbf{r}) = \frac{Ne}{\sqrt{\pi}} \int_0^\infty \frac{\exp[-x^2/(2a^2+t) - y^2/(2b^2+t) - z^2/(2c^2+t)]}{\sqrt{(2a^2+t)(2b^2+t)(2c^2+t)}} dt \tag{A.10}$$

REFERENCES

1. *K. Takayama.* "A New Method for the Potential of a 3 - Dimensional Nonuniform Charge Distribution". Lett. al Nouvo Cimento, vol.34, *N* 7, p.190.
2. *M. Bassetti and G. Erskine.* CERN ISR-TH/80-06 (1980).
3. *S. Myers.* "Review of Beam-Beam Simulations", in: Nonlinear Dynamics Aspects of Part. Acc. Lect. Notes in Phys. V.247, Springer Verlag, (1985), p.176.
4. *A. Chao.* "The Beam-Beam Instability". Lect.at the 3 rd Summer Scholl on High Energy Part. Acc. Brookhaven, (1983).
5. *J.M. Greene*, Proc. of Beam-Beam Interaction Seminar. SLAC, 1980, SLAC-PUB-2624.
6. *J.T. Seeman.* "Observations of the Beam-Beam Interaction", in: Ref. 3, p.121.
7. *B.V. Chirikov.* "A Universal Instability of Multi-Dimensional Oscillator Systems". Phys. Rep.52,(1979), p.263.
8. *A. Gerasimov et al.* "The Dynamics of the Beam-Beam Interaction", in: Ref. 3.
9. *S. Peggs.* "Some Aspects of Machine Physics at CESR", Ph. D. thesis, Cornell University, 1981.
10. *S.V. Milton.* "The Beam-Beam Interaction in Electron Storage Rings: A Study of the Weak/Strong Case". Ph. D.thesis, Cornell University, 1990.
11. *A. Gerasimov et al.* "Nonlinear Resonances and Beam-Beam Effects for Elliptical Beams". Proc. of XIII Int. Conf.

on High Ener. Acc., Novosibirsk, (1986), v.2, p.97.

12. *R.D. Ruth.* "Single Particle Dynamics and Nonlinear Resonances in Circular Accelerators", in: Ref. 3, p.38.
13. *F.M. Izrailev et al.* "Numerical Experiments for a Determination of Stochasticity Criterion in Beam-Beam Interaction". Preprint INP 77-43. Novosibirsk, (1977).
14. *E.D. Curant.* "Beam-Beam Interaction for Bunched and Unbunched Beams". Proc. 11th Int. Conf. on High Ener. Acc. Geneva, (1970), pp.763-766.
15. *F.M. Izrailev.* "Nearly Linear Mappings and their Applications". Phys. 1D, (1980), p.243.
16. *J.L. Tennyson.* "The Instability Treshold for Bunched Beams in ISABELLA", in: Nonlinear Dynamics and the Beam-Beam Interaction, Eds. Month, Herrera.-N.Y.:American Institute of Physics, AIP Conf. Proc. *N* 57, 1979, p.158.
17. *F.M. Izrailev, I.B. Vasserman.* "The Influence of Different Types of Modulations on a Decrease of the Stochasticity Limit in Beam-Beam Effects". Preprint INP 81-60. Novosibirsk, 1981, Proc. of 7th All Union Conf. of Charged Part. Acc., Dubna, 1981, p.288.
18. *S.G. Peggs.* "Beam-Beam Synchrobetatron Resonances". Part. Acc. Conf., Santa Fe, USA, 1983.
19. *S. Krishnagopal, R. Siemann.* "Bunch Length Effects in the Beam-Beam Interaction". Phys. Rev. D, v.41, 1990, p.2312.
20. *N.S Dikansky et al.* "Simulation of Beam-Beam Effects of

Round Beams in Φ-meson Project". Presented on 12th All Union Conf. of High Ener. Acc., 1990.

21. *A.L. Gerasimov et al.* "Beam-Beam Effects with Big Dispersion Function at the Interaction Point", submitted to Nucl. Instr. Meth., September, 1990.
22. *A. Piwinski.* "Synchrobetatron Resonances", in: Ref. 3, p.104.
23. *I.B. Vasserman et al.* Proc. of 7th all Union Conf. on Charged Part. Acc., Dubna, 1981, v.1, p.184.
24. *A.B. Temnykh.* "Influence of Cubic Nonlinearity of Storage Ring Magnetic Field on Beam-Beam Effects on VEPP-4", Proc. of XIII Int Conf. on High Energy Acc., Novosibirsk, 1986, v.1, p.78.
25. *A.B. Temnykh.* "Observation of Beam-Beam Effects on VEPP-4", in: Proc. Third Advanced ICFA Beam Dynamics Workshop on Beam-Beam Effects in Circular Colliders. Novosibirsk, 1989, p.5.
26. *P.M. Ivanov et al.* "Luminosity and Beam-Beam Effects on VEPP-2M with Superconducting Wiggler Magnet", in: Ref.25, p.26.
27. *A.B. Temnykh.* "Phenological Model of Flip-Flop Effect in Colliding Beams". Preprint INP 82-148. Novosibirsk, 1982.
28. *J. Irwin et al.* "The Flip-Flop Effect in Beam-Beam Interaction". Cornell Internal Note, CON 87-15 (1987).
29. *J.L. Tennyson.* "Flip-Flop Modes in Symmetric and Asymmetric Colliding - Beam Storage Rings". Preprint LBL - 28013, 1989.

30. *F. Ruggiero.* "Renormolaised Fokker-Planck Equation for the Problem of the Beam-Beam Interaction in Electron Storage Rings", Annals of Phys., 1984, v.153, p.122.
31. *S. Kheifets.* "Study of a Weak Beam Interaction with a Flat Strong Beam", Part. Accel., 1984, v.15, p.153.
32. *J.F. Schonfeld.* "Statistical Mechanics of Colliding Beams", Annals of Phys., 1985, v.160, p.149.
33. *A.L. Gerasimov.* "Phase Convection and Nonequilibrium Fluctuations in Nearly-Integrable Systems". Phys. Lett. A, V.135, 1989, p.92.
34. *A.L. Gerasimov.* "Phase Convection and Distribution 'Tails' in Periodically Driven Brownian Motion". Phys. D, V.41, 1990, p.89.
35. *Y.H. Chin.*"Renormalization Theory of Beam-Beam Interaction in Electron-Positron Colliders", in: Ref.25, p.69.
36. *H. Risken.* "The Fokker-Planck Equation". Springer, Berlin, 1983.
37. *A. Ventzel and M. Freidlin.* "Random Perturbations of Dynamical Systems". Springer, Berlin, 1984.
38. *J.L. Tennyson.* "Resonance Transport in Near Integrable Systems with Many Degrees of Freedom". Physica D, 1982, v.5, p.123.
39. *G.N. Kulipanov et al.* "Influence of Nonlinearities on Betatron Oscillations in Storage Ring". Preprint INP-251, Novosibirsk, 1968.

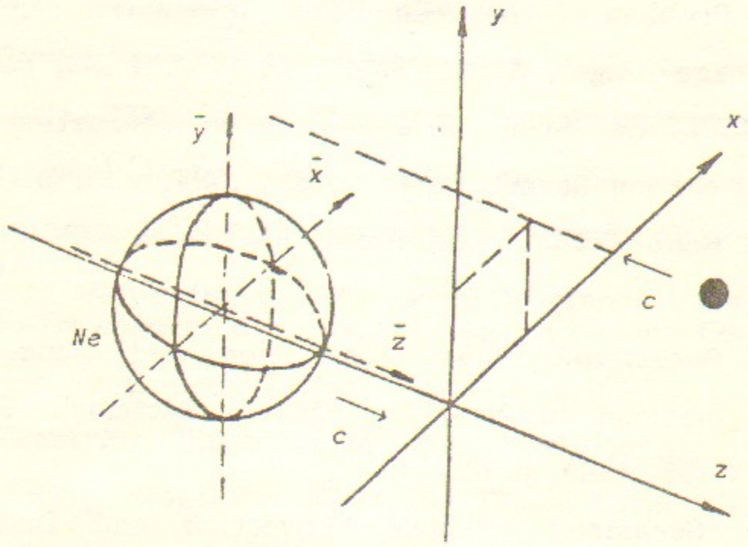

Fig. 1. The coordinate systems.

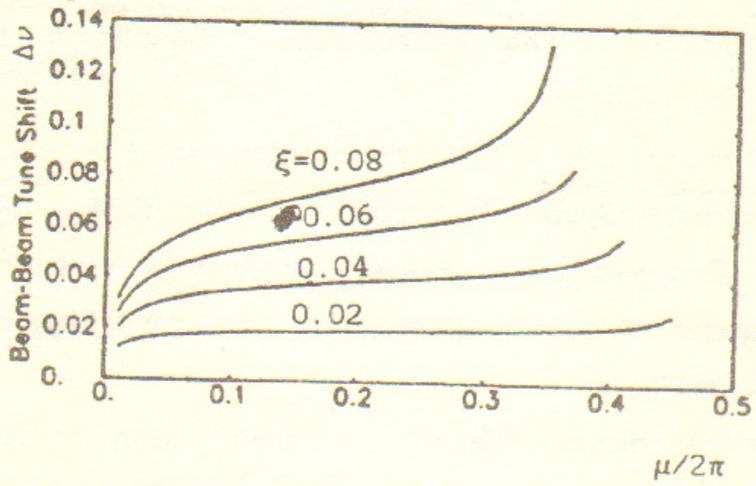

Fig. 2. Tune shift dependence on ξ and μ.

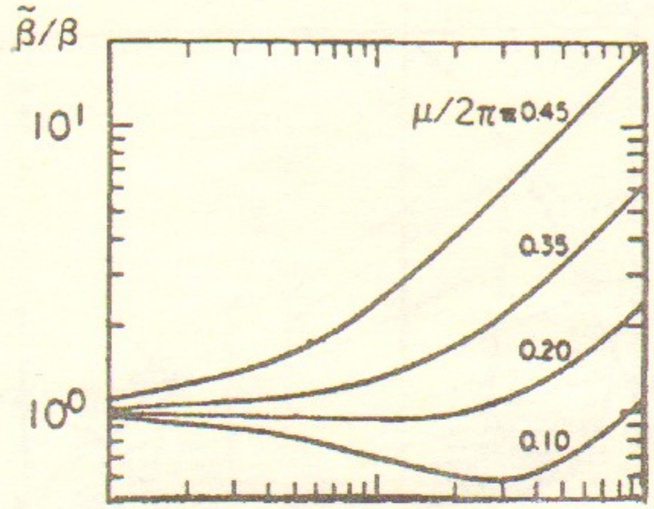

Fig. 3. The dynamic beta effect: μ is the unperturbed phase advance between collision points.

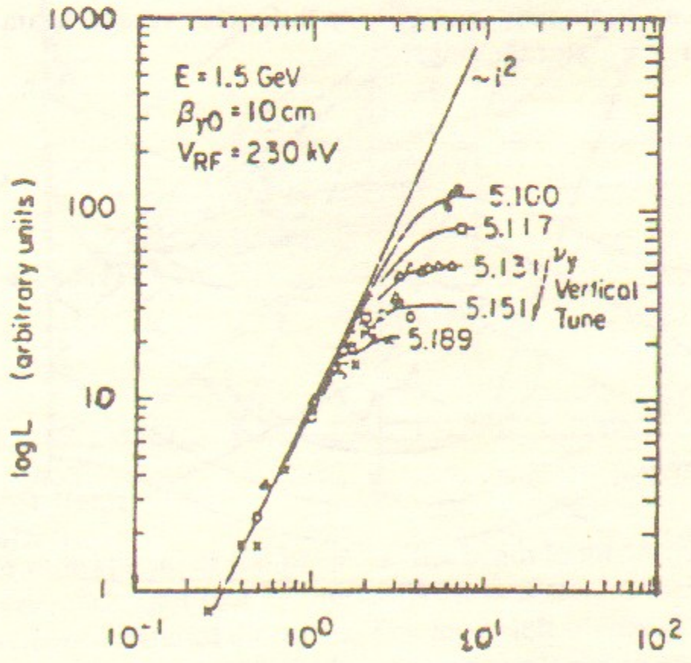

Fig. 4. SPEAR I data that show tune and beam intensity dependencies of luminosity.

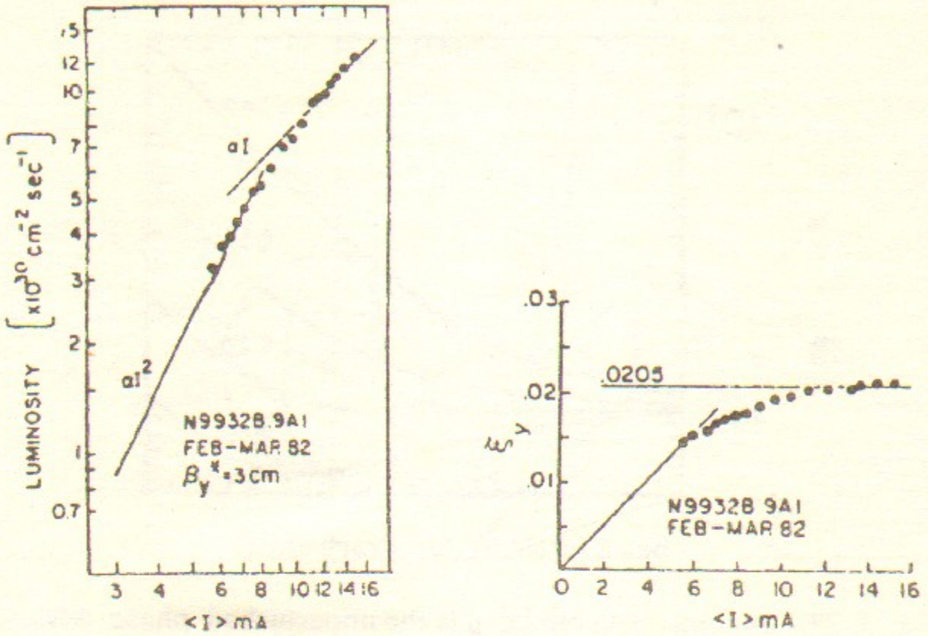

Fig. 5. Typical luminosity and ξ_y dependencies versus beam intensity for most e^+e^- storage rings.

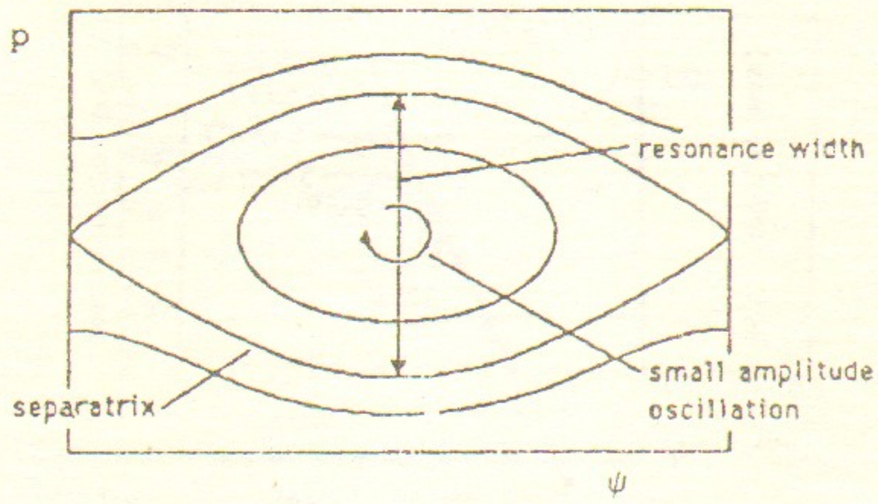

Fig. 6. Nonlinear resonance in phase space.

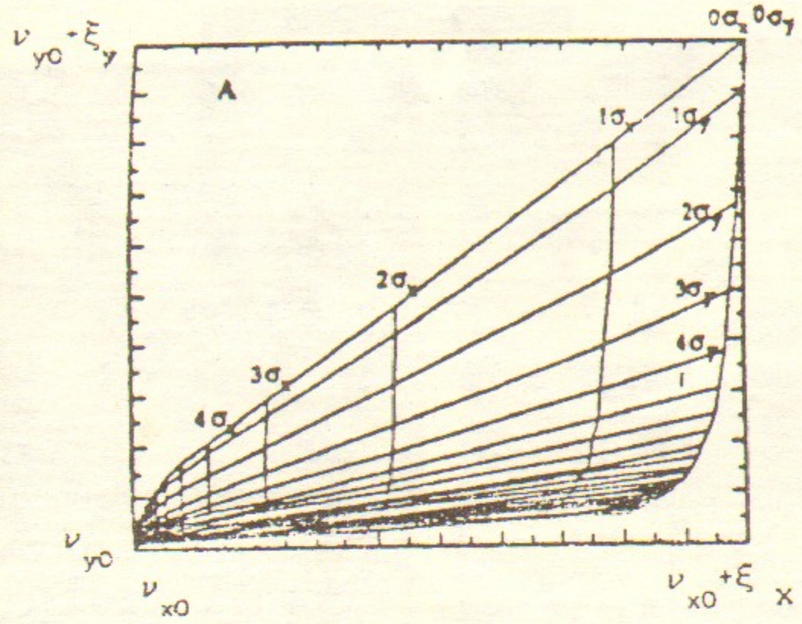

Fig. 7. *A*) The tune spread of the beam, or the beam footprint. The spacings between each grid line in the footprint is a step of 1σ in either the vertical or horizontal direction. The lower left corner of the footprint is at the machine tune. *B*) The footprint placed in the tune plane amongst the resonances.

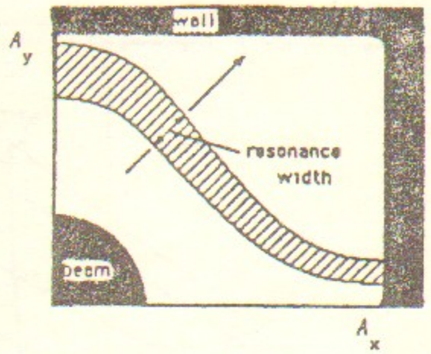

Fig. 8. Nonlinear resonance in the amplitude plane.

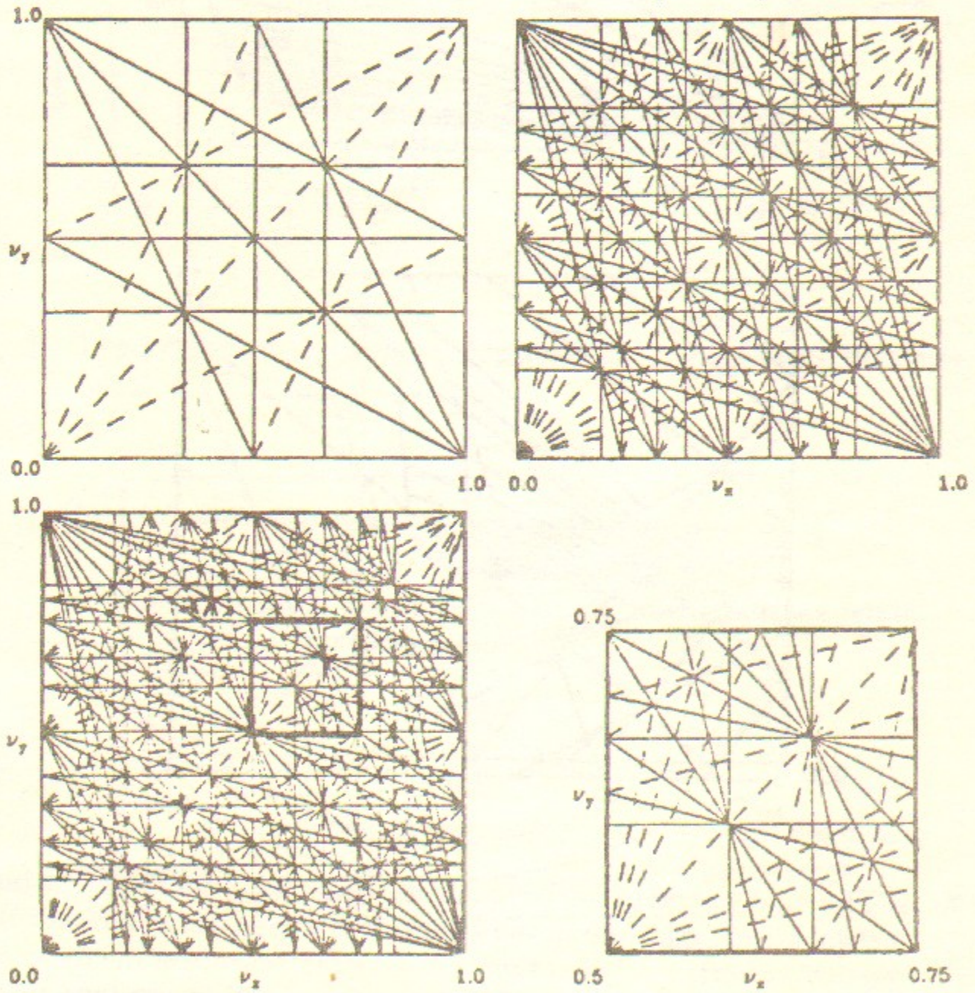

Fig. 9. Resonance lines in tune space. The figures include $|l| + |m| \leq 3$, 5 and 6. The outlined area in the sixth order case is blown up to show detail.

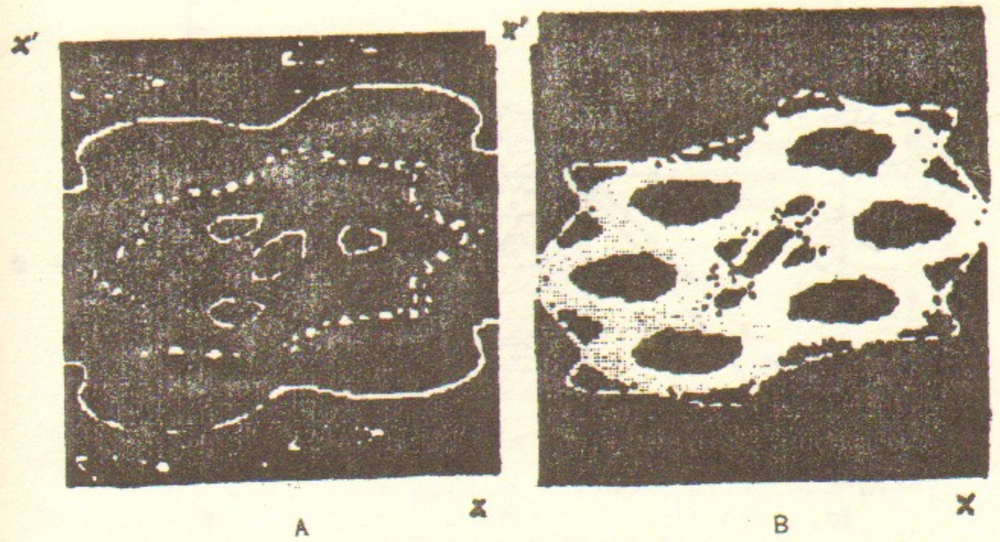

Fig. 10. Phase space plot of a particle motion. Figure *A* is the example of the regular (stable) motion. Parameter ξ is chosen below the treshold, determined by overlap condition of the isolated resonances. Figure *B* is the example of the irregular (unstable) motion. Here parameter ξ is chosen over the threshold.

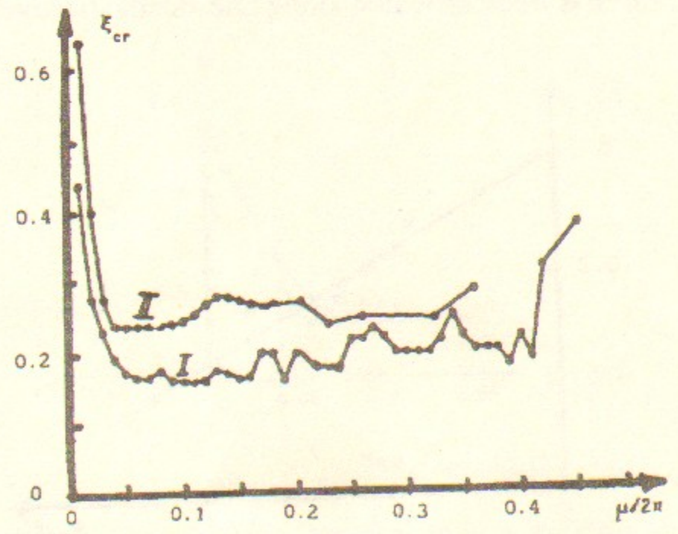

Fig. 11. The stochasticity threshold ξ_{cr} versus the fraction part of the betatron phase advance between interactions. Line I is a round beam case, line II is a flat beam case.

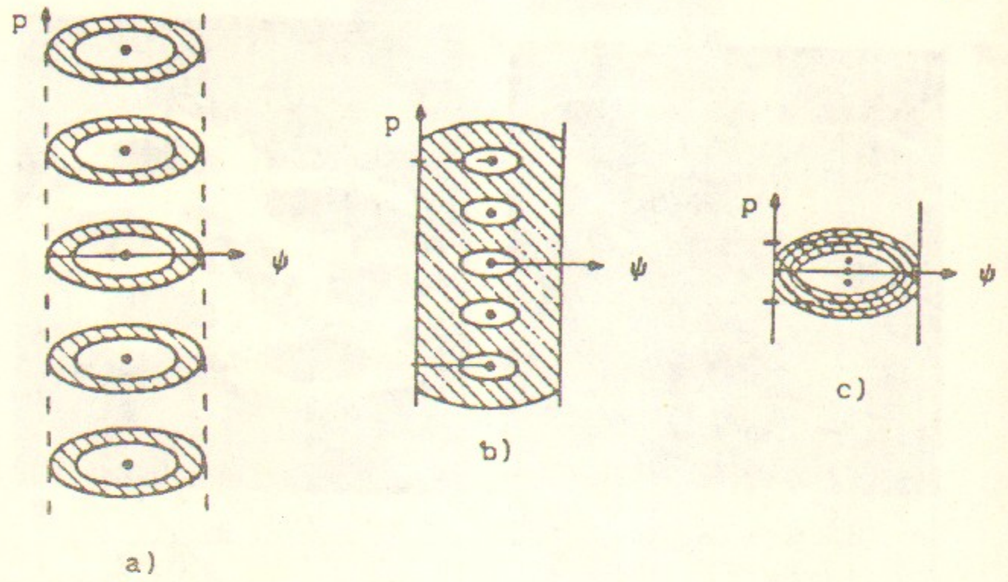

Fig. 12. Three regimes of the motion inside the synchrobetatron resonance multiplet. *a)* Large modulation: the resonances do not overlap, there is a weak diffusion along the separate stochastic layer; *b)* intermediate modulation: there is a strong diffusion along the wide stochasticity region; *c)* small modulation: all resonances merge in one, there is weak diffusion along one stochastic layer.

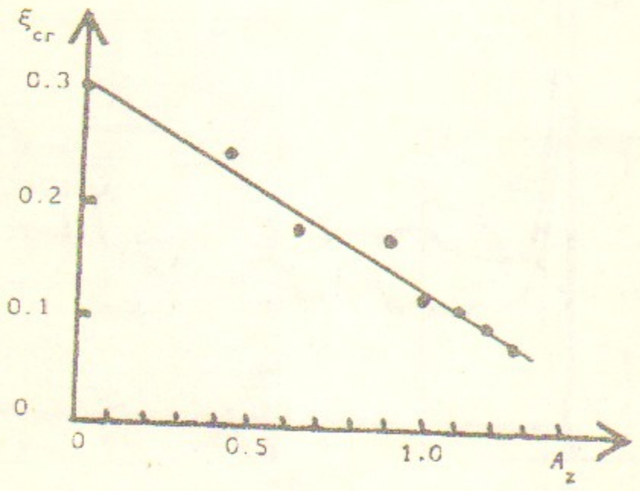

Fig. 13. The critical value ξ_{cr} dependence on the normalized amplitude of synchrotron oscillations, A_z.

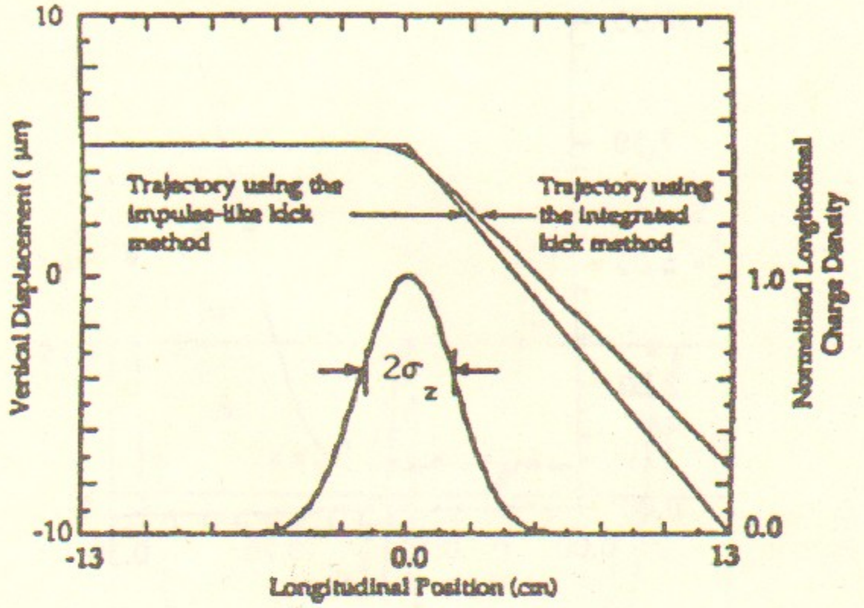

Fig. 14. The trajectory of $1\sigma_y$ particle as it passes through the opposing beam. Two cases are shown: the pancake-like case and smooth integrated kick case. The deflection of the trajectory produced by the integrated kick is less than that of the impulse-like case. The longitudinal distribution (Gaussian) of the opposing bunch is shown for reference.

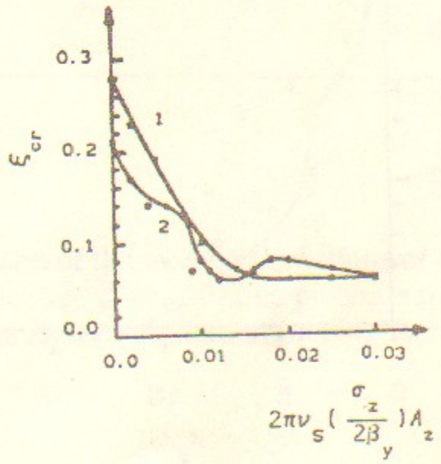

Fig. 15. The critical value ξ_{cr} dependence on the amplitude of the tune modulation. Line 1 represents a flat beam; line 2 does so for a round beam.

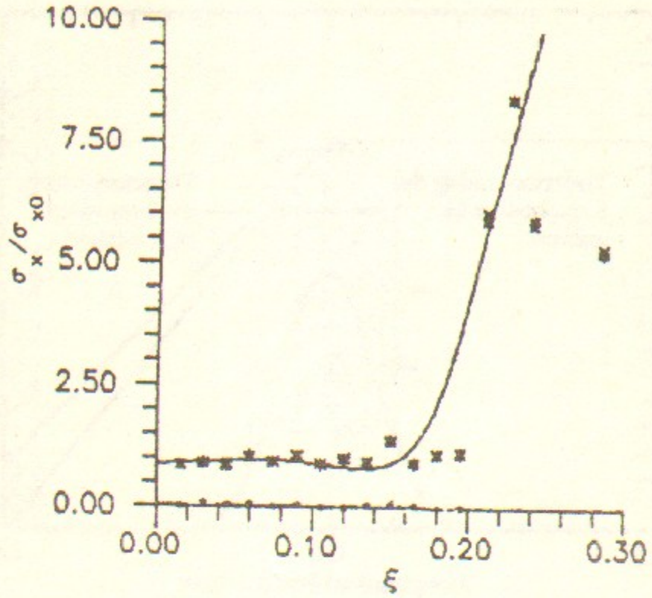

Fig. 16. The dependence of the beam size on the parameter ξ. The simulation was carried out at $\sigma_z/\beta_y = 0.83$, $\nu_x = \nu_y = 0.08$ and $\nu_s = 0.02$.

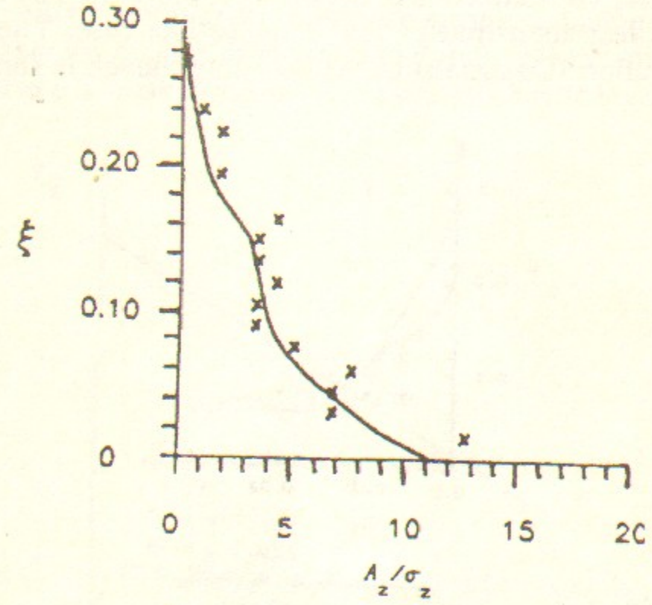

Fig. 17. The dependence of the maximal value of ξ on the amplitude of the longitudinal oscillation. The simulation was carried out at $\sigma_z/\beta_y = 0.83$, $\nu_x = \nu_y = 0.08$ and $\nu_s = 0.02$.

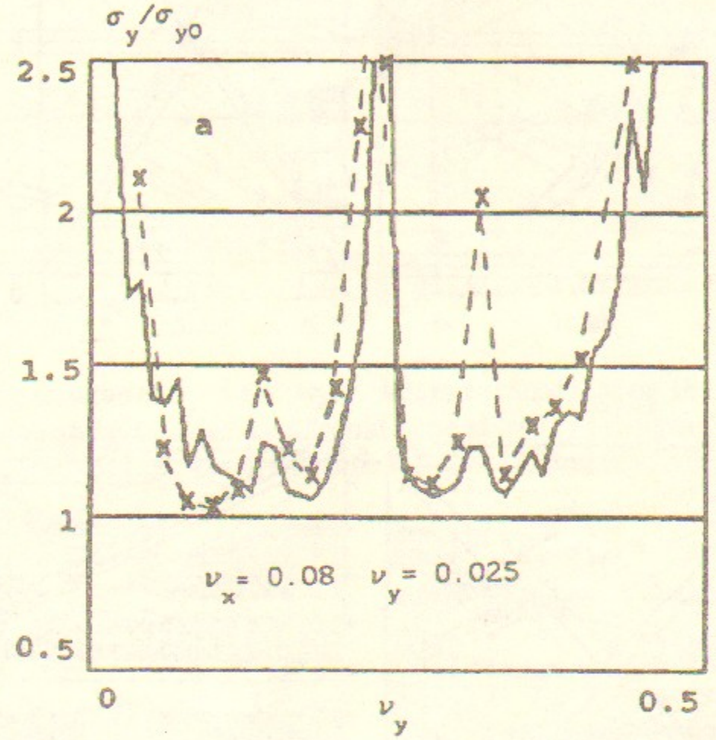

Fig. 18. The comparison of the model calculations of the 'weak' beam vertical size with tracking. The solid line presents the model prediction, the dotted line presents the simulation results.

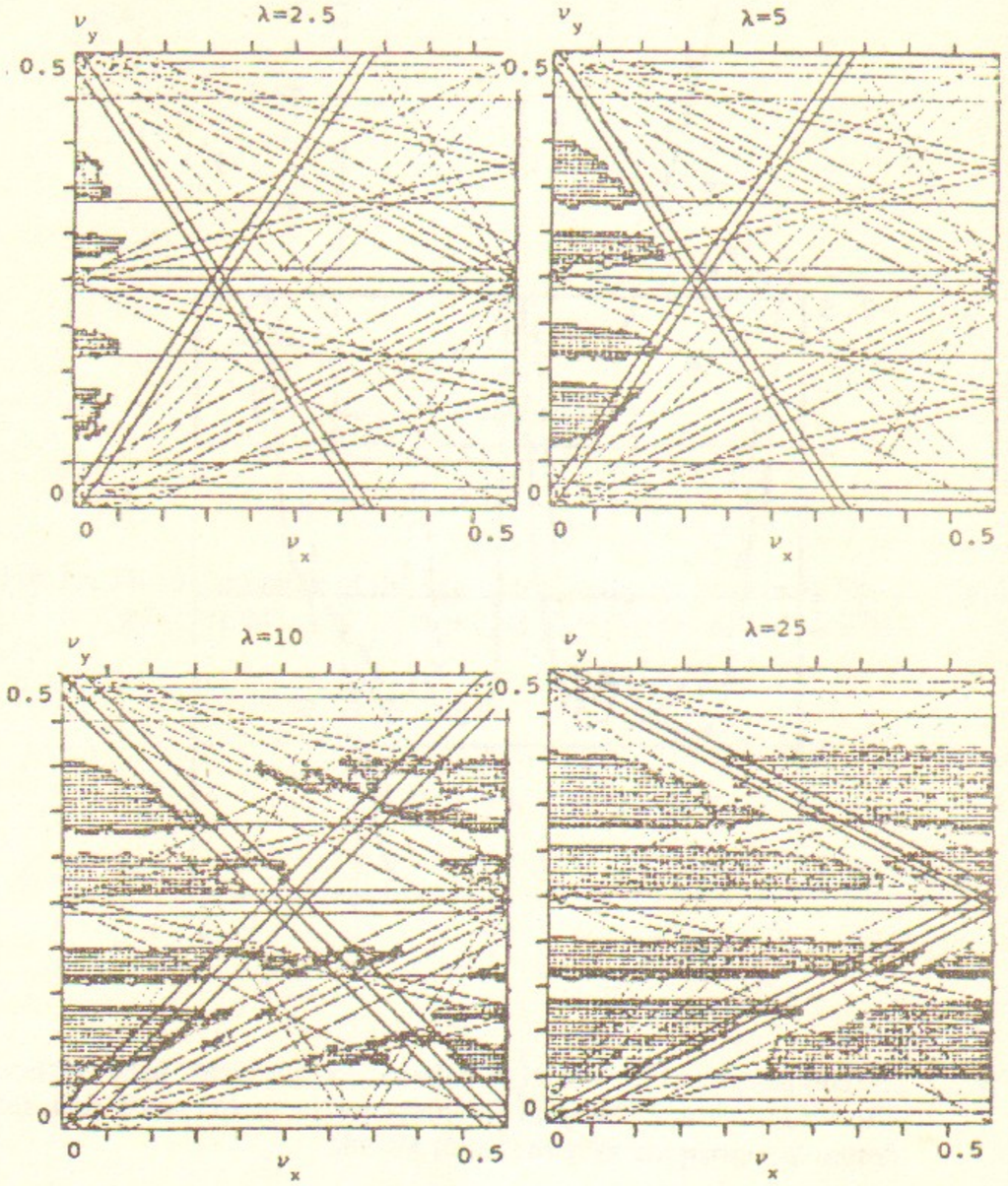

Fig. 19. The contour plot of the areas of tunes, where the blow-up of the 'weak' beam vertical size does not exceed 15%. These areas are marked with shading. Four cases with $\lambda = 2.5$, $\lambda = 5$, $\lambda = 10$ and $\lambda = 25$ are shown. On the every plot all reonances up to six order with $|l| \leq 3$ are presented.

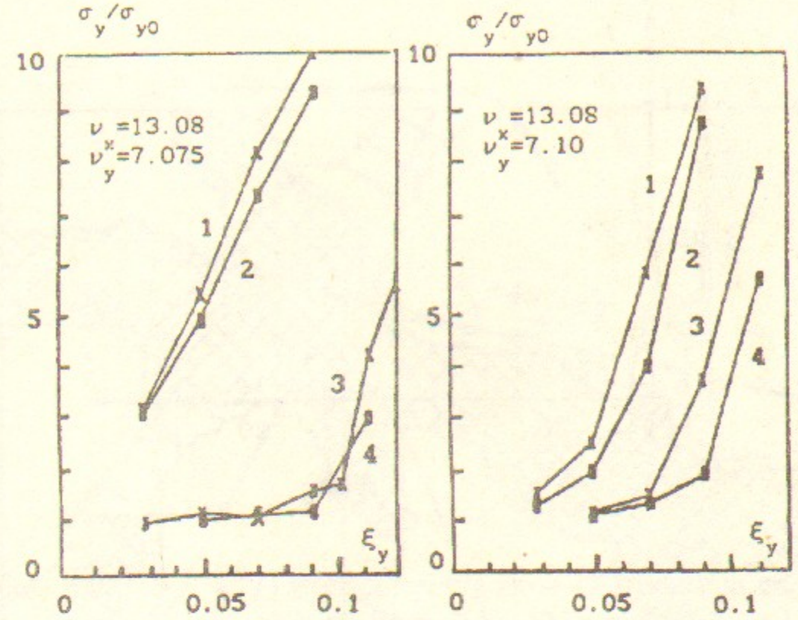

Fig. 20. The dependence of the 'weak' beam vertical size on the vertical linear tune shift ξ_y. The horizontal tune shift ξ_x is satisfied the condition $\xi_x = \xi_y/5$. Line 1— $\lambda = 0$, line 2— $\lambda = 0.7$, line 3— $\lambda = 5$, line 4— $\lambda = 25$.

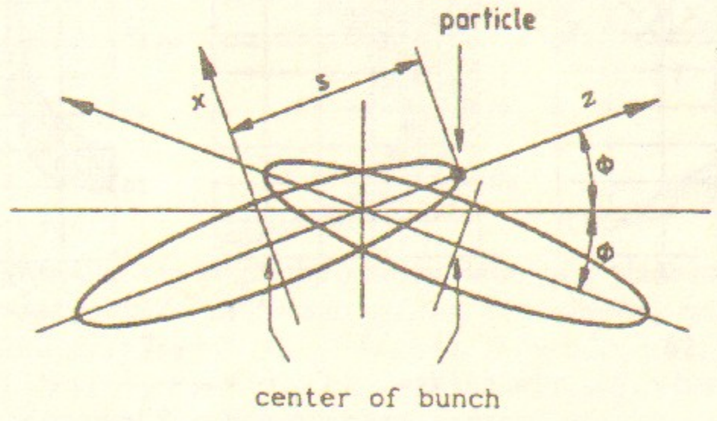

Fig. 21. Beam-beam interaction at a crossing angle.

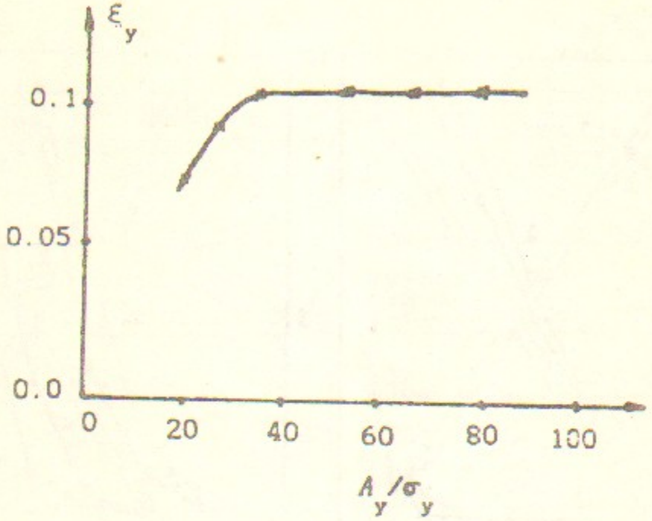

Fig. 22. The maximum ξ_y versus the aperture (VEPP-2M, 0.5 GeV, 'weak-strong' beams, $\sigma_y \ll \sigma_x$, $\beta_x = 40$ cm, $\beta_y = 3$ cm).

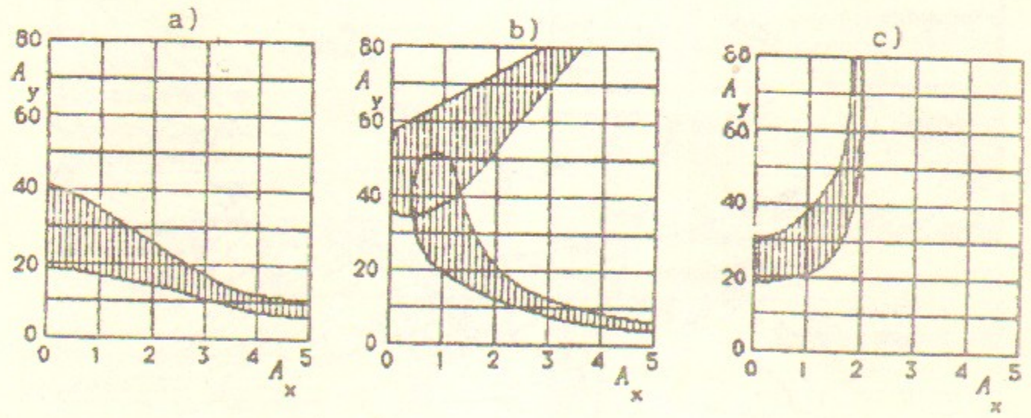

Fig. 23. The resonance $10\nu_y = 96$ in amplitude plane for the cases: *a*) with zero machine nonlinearity, *b*) with positive nonlinearity, *c*) with negative nonlinearity.

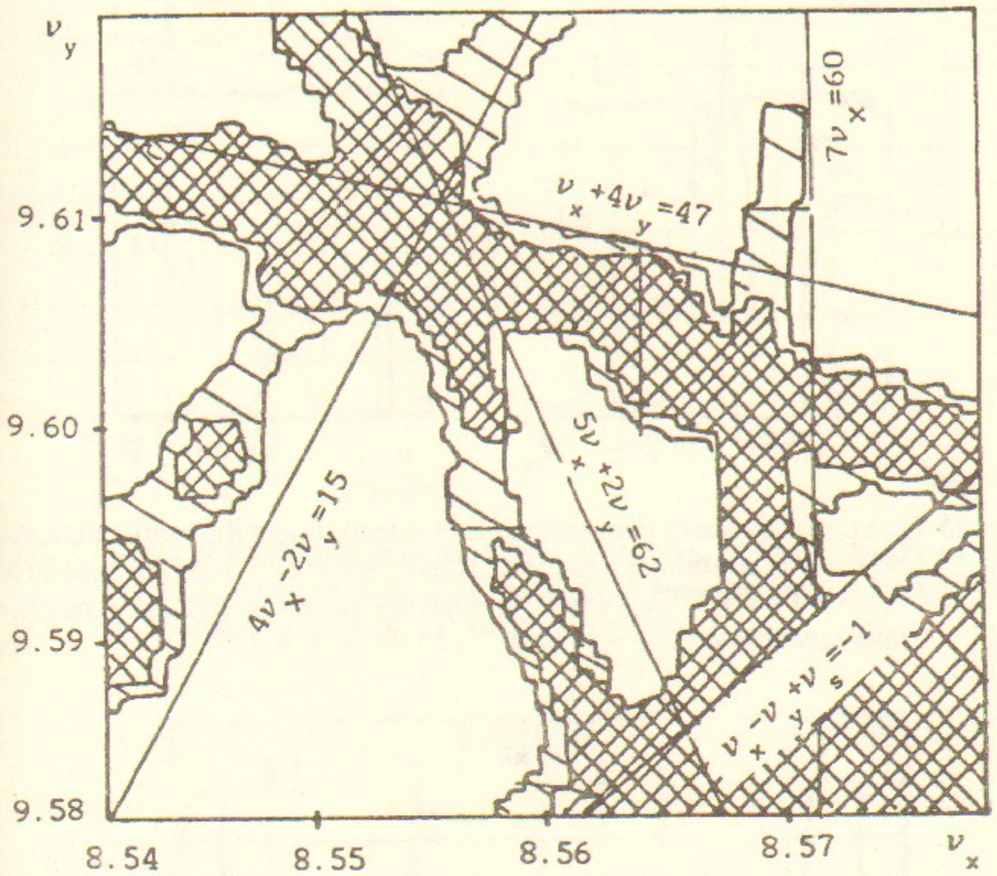

Fig. 24. Positron loss rate versus the position on the tune plane near the main working point of VEPP-4 storage ring. The following resonances are identified: *1*) $7\nu_x = 60$, *2*) $\nu_x + 4\nu_y = 47$, *3*) $5\nu_x + 2\nu_y = 62$, *4*) $4\nu_x - 2\nu_y = 15$, *5*) $\nu_x - \nu_y + \nu_s = -1$. There was the orbit separation $\sim 0.1\sigma_x$ in the horizontal direction during the experiment.

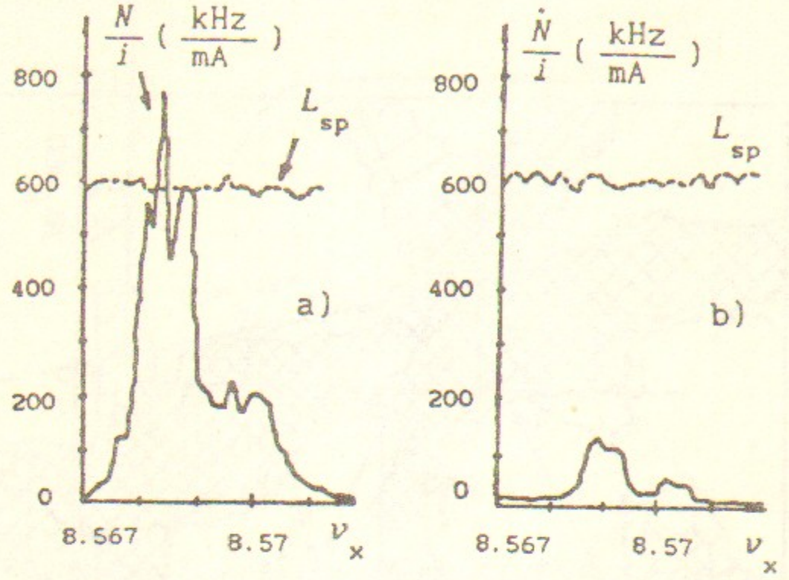

Fig. 25. The dependence of the positron loss rate and specific luminosity, L_{sp}, on the horizontal betatron tune during the scan across the resonance $7\nu_x = 60$ on VEPP-4 with the opposite values of the cubic machine nonlinearity: *a*) $R_x \cong 6.9\ \text{cm}^{-1}$, *b*) $R_x \cong -6.9\ \text{cm}^{-1}$.

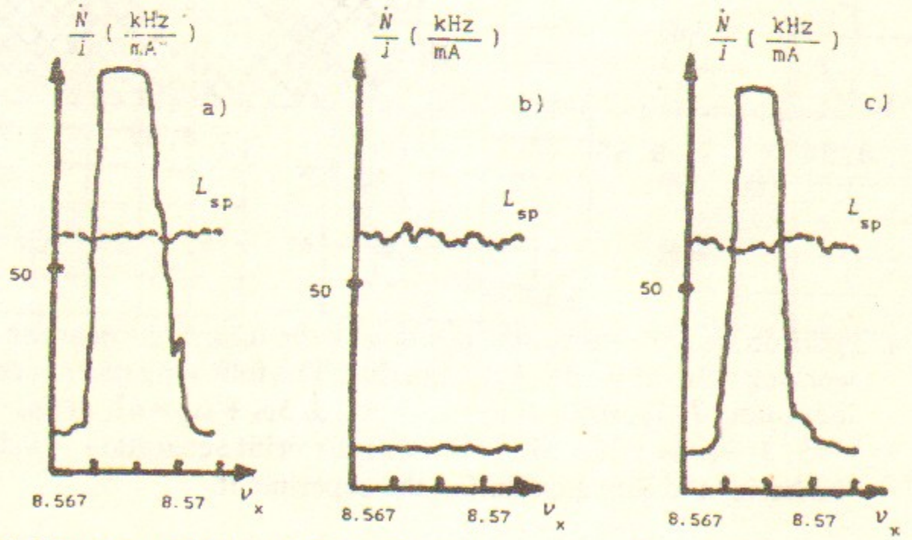

Fig. 26. The dependence of the positron loss rate and specific luminosity, L_{sp}, on the horizontal betatron tune during the scan across the resonance $7\nu_x = 60$ on VEPP-4: *a*) orbit separation is $-0.1\sigma_x$, *b*) zero orbit separation, *c*) orbit separation is $0.1\sigma_x$.

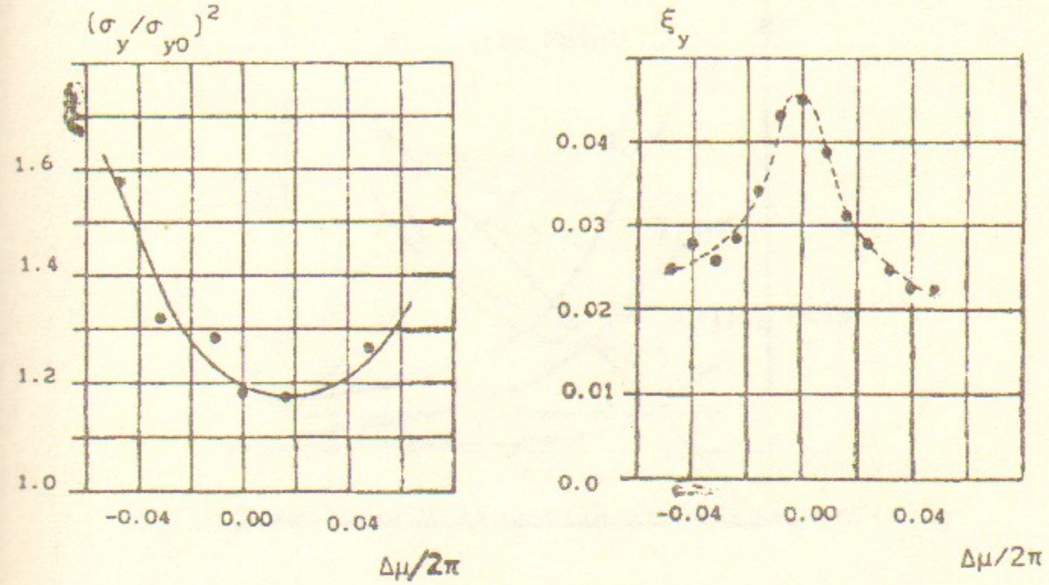

Fig. 27. Vertical emittance and maximal ξ_y versus the asymmetry of the vertical betatron phase advance between the interaction points (VEPP-2M, 510 MeV, $\nu_x = 3.059$, $\nu_y = 3.097$).

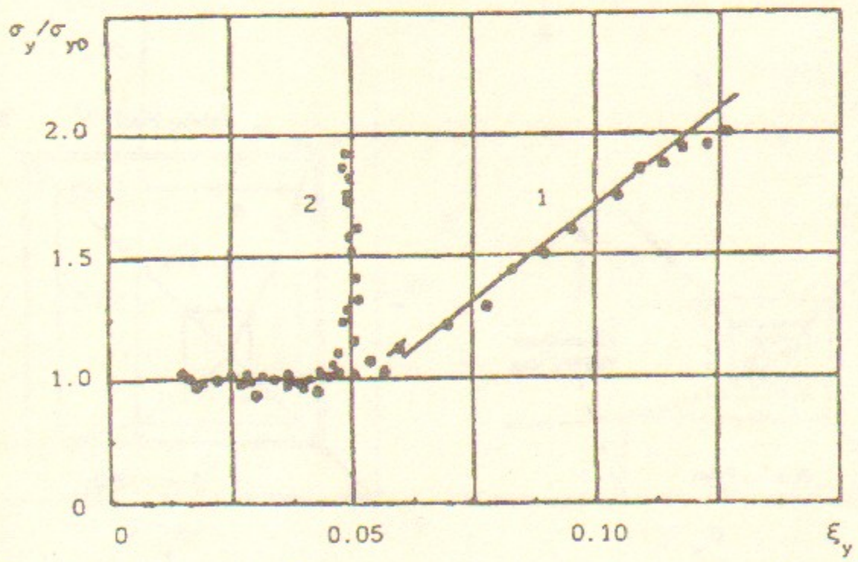

Fig. 28. Vertical beam size blow up versus the attained value of ξ_y. Case 1 – $i^+ << i^-$, case 2 – $i^+ = i^-$. (VEPP-2M, $E = 510$ MeV, $\beta_y/\sigma_z = 2.5$, $\nu_x = 3.054$, $\nu_y = 3.087$).

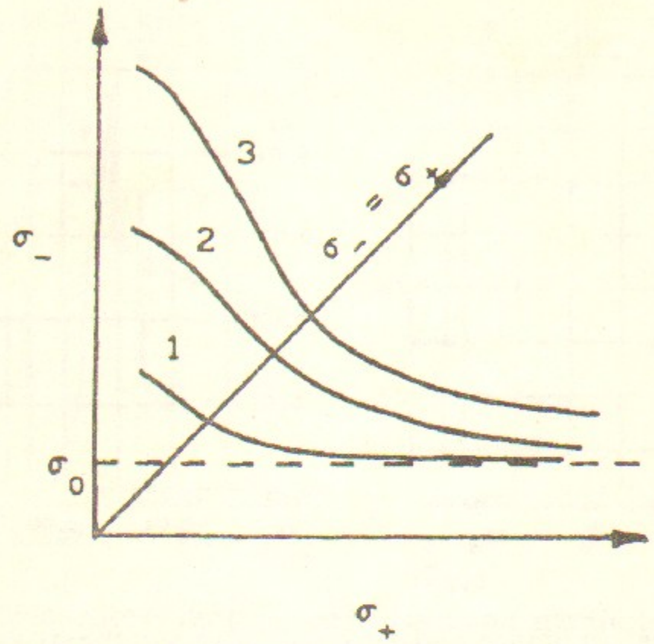

Fig. 29. Behaviour of one beam size as a function of the opposite beam size. Line $1 - i^+ = i_0$, line $2 - i^+ = 2i_0$ and line $3 - i^+ = 3i_0$.

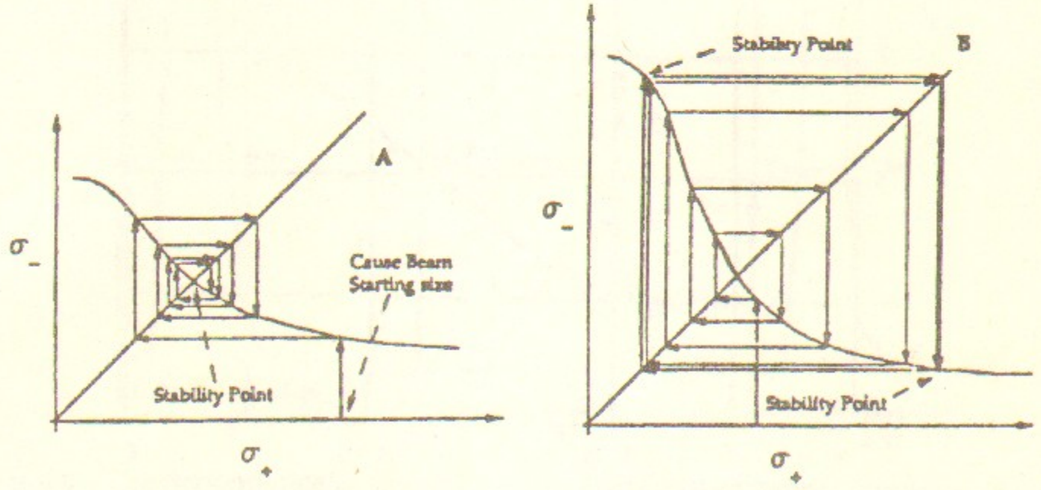

Fig. 30. A) The path to equal beam sizes, *B*) the path to flip-flop.

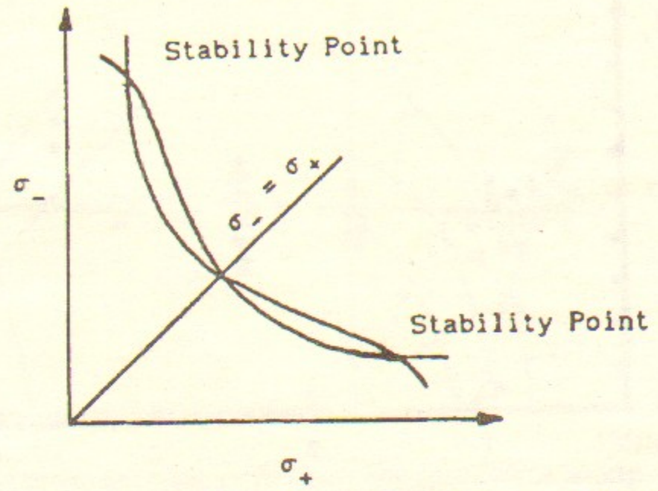

Fig. 31. The system (10.1) above the critical condition (10.2).

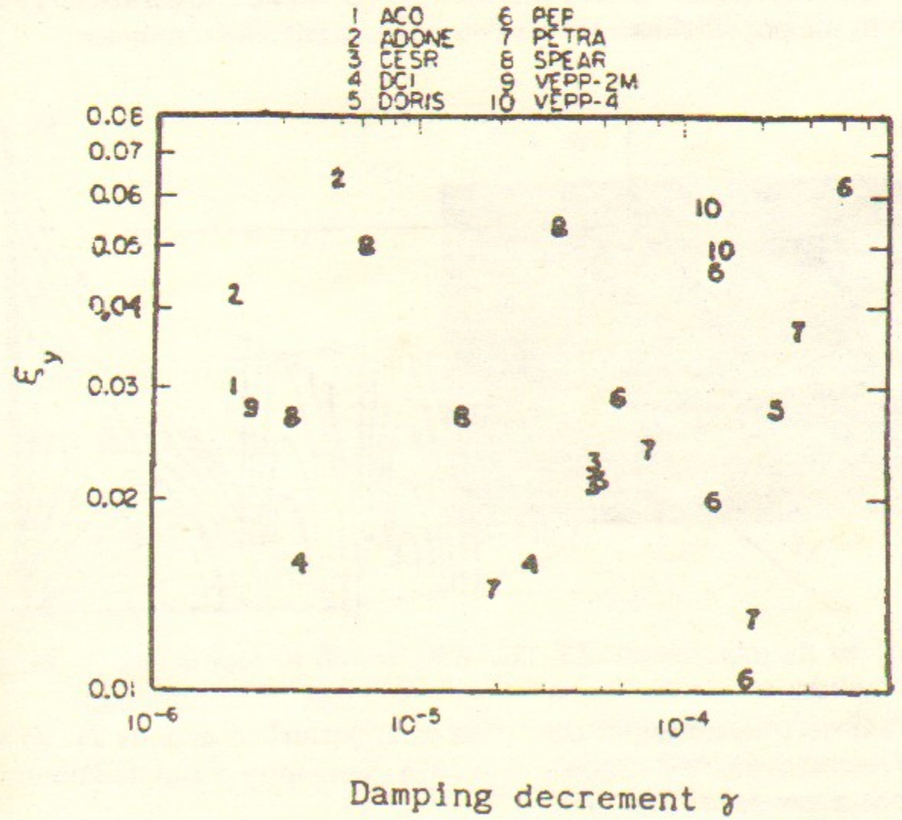

Fig. 32. The maximal ξ_y versus damping decrements observed on the various machines. (Reproduced from Ref. 6).

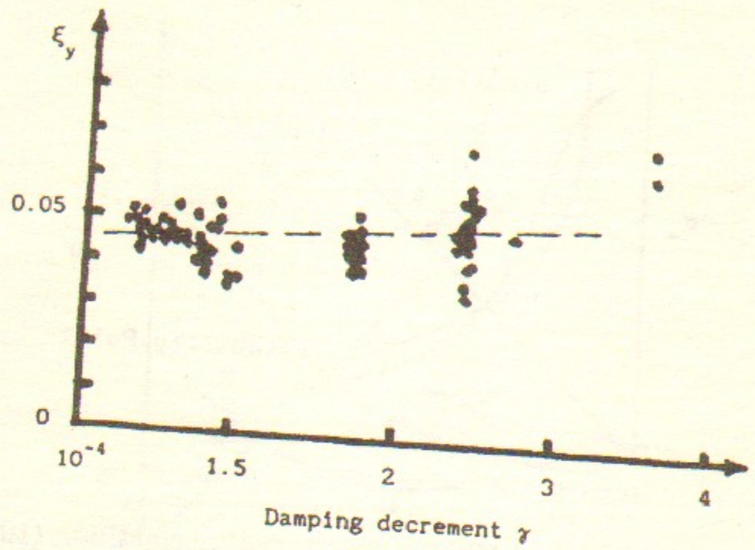

Fig. 33. The dependence of maximal value ξ_y from the damping decrement. The experimental data obtained on VEPP-4 during the energy scan in the physic runs.

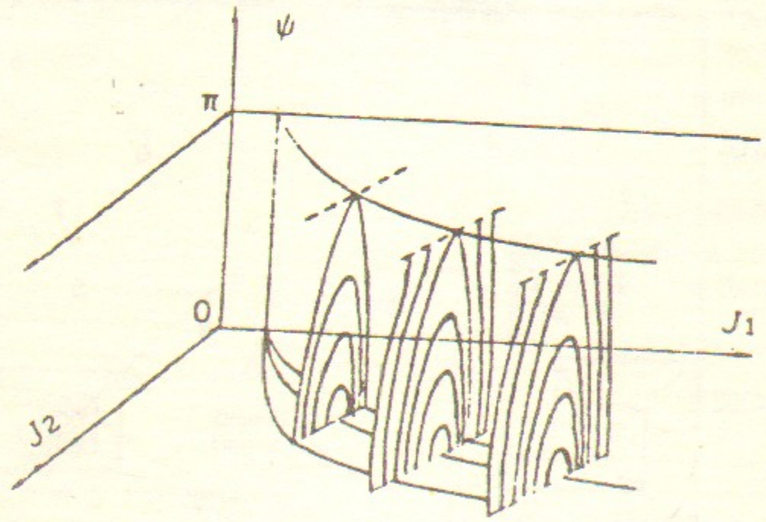

Fig. 34. Phase trajectories in the space of unperturbed actions J_1, J_2 and resonant phase $\psi = l\Phi_x + m\Phi_y - k\theta$ in the vicinity of isolated nonlinear resonance.

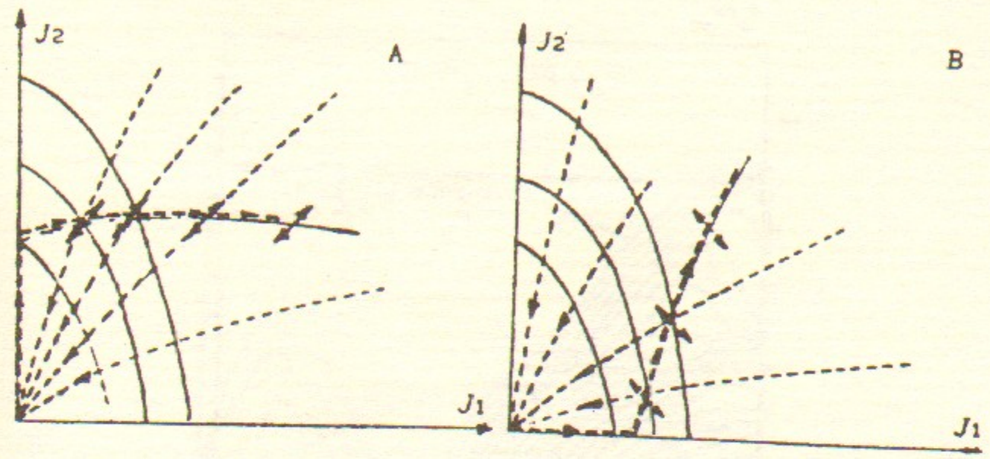

Fig. 35. Case *A* is the extreme path along the resonance 'along damping'. Case *B* is the extreme path along the resonance line 'against damping'. The dashed lines show the unperturbed motion with damping; the fat dashed line denotes the extreme path; the fat solid line is the resonance line; the small arrows are the oscillations at the resonance.

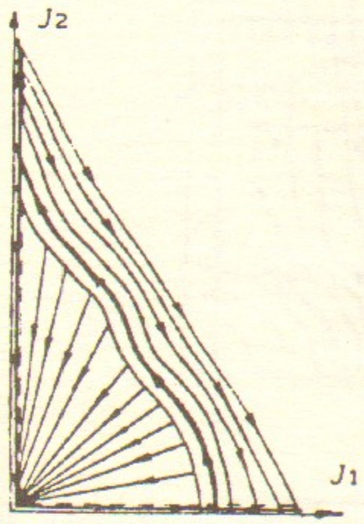

Fig. 36. Distributions of fluxes in the plane J_1, J_2.

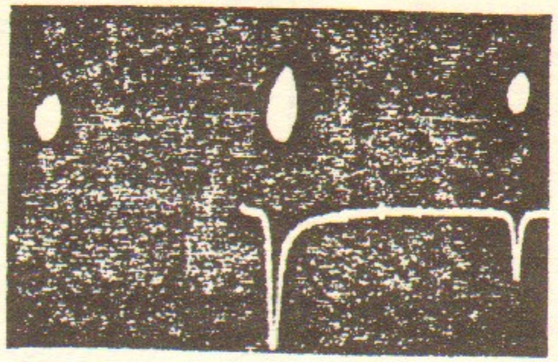

Fig. 37. TV representation of the beam transverse cross-section and the oscillogram of the particle density distribution. The vertical betatron tune is chosen near the fourth order resonance $4\nu_y = 3$.

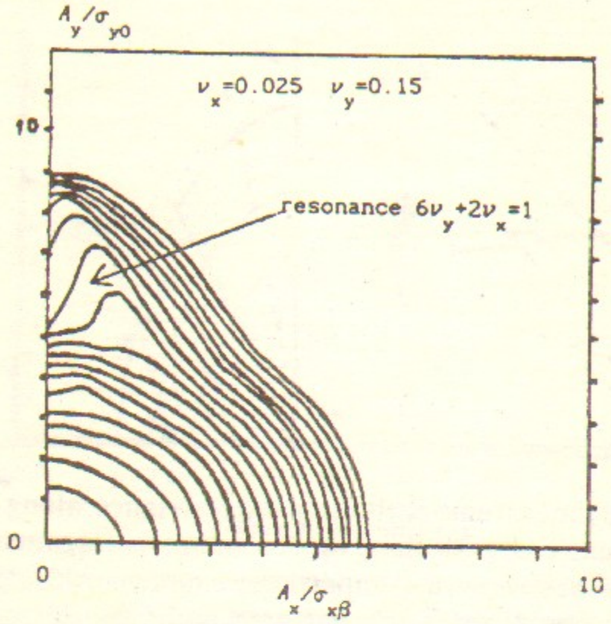

a)

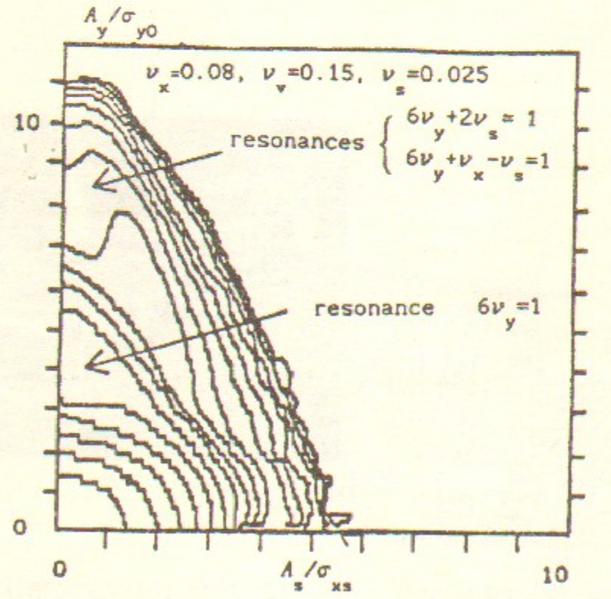

b)

Fig. 38. The contour plot of the particle density distribution function $\rho(A_x, A_y)/A_x \cdot A_y$. The level lines show the exponential reduction of the particle density with the factor *e*. Case *a*) is the model calculations. Case *b*) is the result of the simulation. The effect of the tune modulation is not included into the simulation.

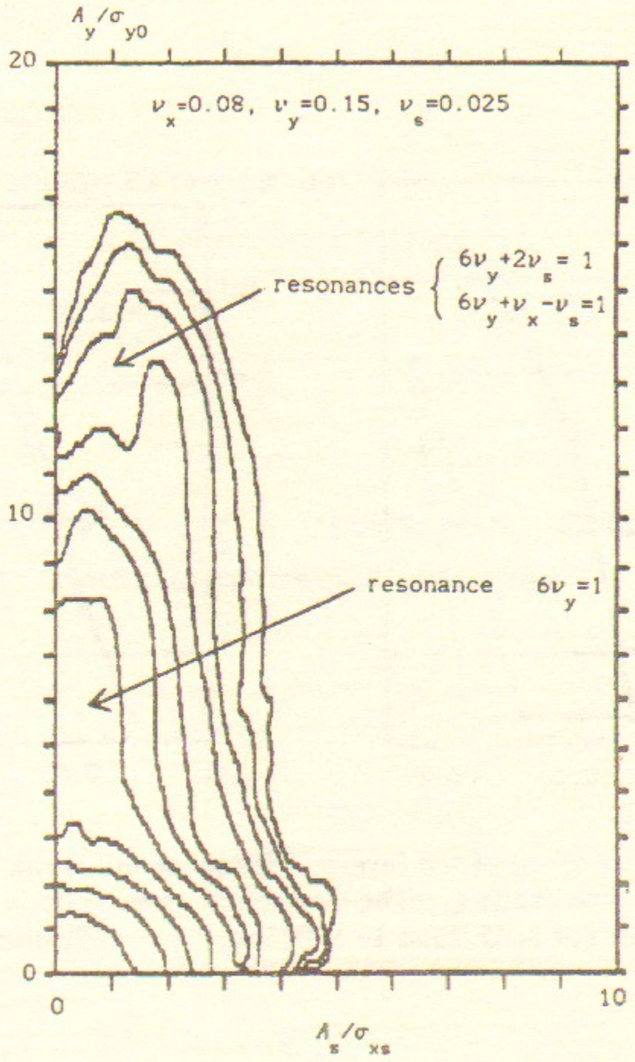

Fig. 39. The same as in the Fig. 38*b* and with the effect of tune modulation included into the simulation.

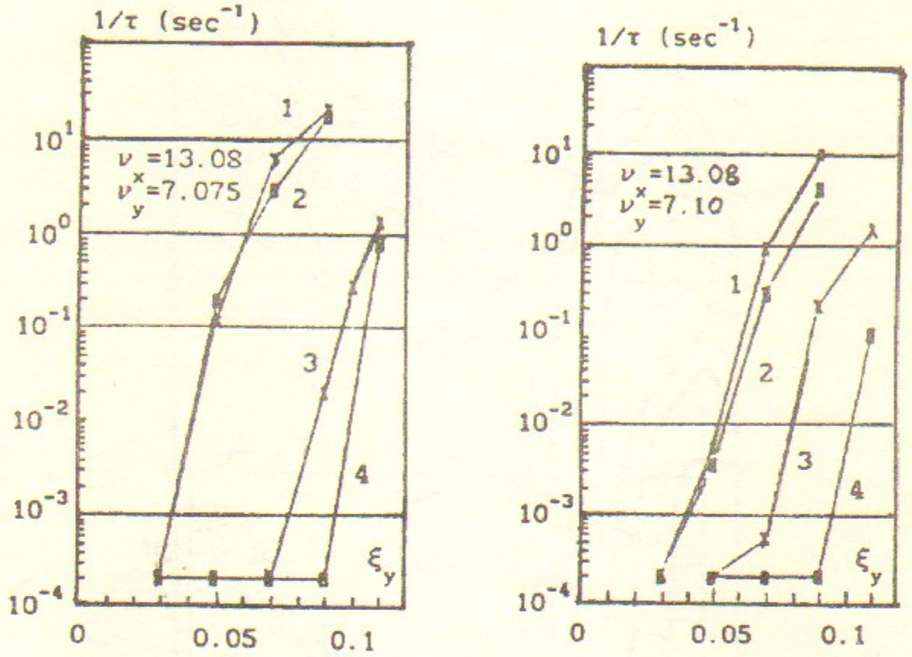

Fig. 40. The dependence of the inverse lifetime of the 'weak' beam on the vertical tune shift ξ_y. The horizontal tune shift is satisfied the condition $\xi_x = \xi_y/5$. Line 1 – λ=0, line 2 – λ=0.7, line 3 – λ=5, line 4 – λ=25.

A. A. Zholents

Beam-Beam Effects in Electron-Positron Storage Rings

А. А. Жоленц

Эффекты встречи в электрон-позитронных накопительных кольцах

Подписано в печать 18 февраля 1991 г.
Формат бумаги 60X90 1/16.
Объем 3,7 печ. л., 3,0 уч-изд. л
Тираж 250 экз. Бесплатно. Заказ N 18.

Ротапринт ИЯФ СО АН СССР, г. Новосибирск, 90.